Image Texture Tools

Texture Synthesis, Texture Transfer,
and Plausible Restoration.

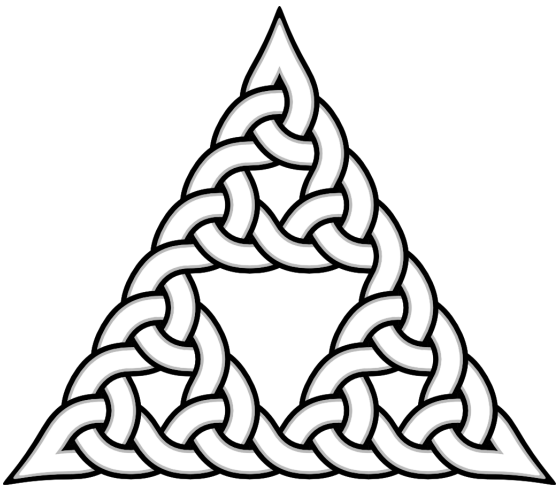

Paul Francis Harrison

Clayton School of Information Technology,

Monash University

2005

Contents

Abstract

Three image texture operations are identified: **synthesis** of texture from a sample, **transfer** of texture from one image to another, and **plausible restoration** of incomplete or noisy images. As human visual perception is sensitive to details of texture, producing convincing results for these operations can be hard. This dissertation presents several new methods for performing these operations. With regard to texture synthesis, this dissertation presents a variation on the best-fit method [Efros and Leung, 1999, Garber, 1981] that eliminates the "skew" and "garbage" effects this method sometimes produces. It is also fast, flexible, and simple to implement, making it a highly practical method. Also presented is a simple and fast technique based on random collage. Both of these techniques can be adapted to transfer texture from one image to another. Next, a noise removal method that is guided by a model of an image's texture, in the form of a non-linear predictor, is presented. The method is applied to plausibly restoring the texture of images degraded by compression techniques such as palettization (e.g. GIF), and to the removal of Gaussian noise, with results comparable to state-of-the-art wavelet-based methods. Finally, a more abstract form of texture synthesis is examined, based on the arrangement of tiles of specified shape. This is used to show the origins of the artifacts seen in best-fit synthesis.

Declaration

I, Paul Harrison, declare that this thesis contains no material which has been accepted for the award of any other degree or diploma in any university or other institution and to the best of my knowledge contains no material previously published or written by another person, except where due reference is made in the text of the thesis.

Paul Harrison

Acknowledgements

I thank my supervisor, Dr. Alan Dorin, not least for forcing me to learn how to write. I thank Dr. Peter Tischer for a number of helpful criticisms of this work. I also thank the authors of various pieces of free software—The GIMP, Python, Numeric Python, Latex, and others—without which this thesis would have been considerably harder to complete.

Chapter 1

Introduction

This dissertation describes a number of new tools for working with texture within the domain of digital images.

It is an easily observed trait that we surround ourselves with texture far beyond the need of function. Before the modern fashion for austere perfection, architecture was routinely decorated with intricate patterns [Fearnley, 1975]. We surround ourselves with interestingly textured objects and images. Our brains are wired to analyze texture at the lowest levels of processing (Section 2.1).

There is a gap between our desire for textured objects and the ability of computer-based design tools to craft texture well. These tools represent structure using piecewise continuous functions: polygons, spline curves, smooth gradients of colouration, and so on. They therefore afford the design of smoothly perfect objects over objects who's design is partly dictated by the logic of their texture. A "texture" may be applied to the surface of some designed object, but such texture does not interact with the structure of the object being designed. Compare this to chiseling wood or painting a canvas, where the nature of the material influences the form of the final product.

The word "texture" is peculiar for being applied to many different kinds of thing. To make any progress, a specific definition is required. The definition used in this dissertation is that texture is the localized rules of arrangement of parts that remain consistent throughout an object. These local rules may give rise to large scale form, but the rules themselves should refer only to small areas. Mathematically, these rules may be treated as a Markov Random Field (Section 2.2.2).

This definition allows for complex textures in ways that may not at first be apparent. A texture by this definition may be composed of a number of sub-textures, so long as the sub-texture a local area belongs to can be determined just by looking at that local area. Such a texture will also have rules for transitions between different sub-textures.[1] It is also possible, and common, for complex large features to emerge from simple local rules. An example of this is shown on the title page (see Section 7.4.2).

This definition of texture allows a range of operations, which are usually considered separate, to be seen as instances of a small number of operations on textured objects. Three types of operation are examined in this dissertation:

1. We might **synthesize** objects of the same texture as a given object. These creations could inherit desirable properties present in the original.

2. If we have only part of an object, or if it has been damaged, we might try to find a **plausible restoration** of its original form by reference to its texture. For example, we might try to fill in gaps[2]

[1] This bears some similarity to modulation between keys in music. As in music [Keys, 1961, pp. 99], the exact boundary between two regions may be somewhat fuzzy.

[2] Filling in of gaps is often referred to as "interpolation". However interpolation has a connotation of smoothness, perhaps restoring features such as edges but usually not preserving any roughness of texture. Such smoothness is actually quite *implausible*,

or correct inaccuracies of measurement, or we might try to infer the future evolution of a thing changing over time. A restoration is *plausible* if it conforms to what is known of the object's texture.

3. In art, a likeness of an object may be made with a different texture to the original. This is called **texture transfer**. For example, an artist might make a likeness of some object in stone or paint.

This thesis describes ways to perform these three types of operation on digital images (see Figure 1.1). The focus is on working with existing texture (with the exception of Chapter 7, which looks at creating new textures). For digital images:

1. Synthesis, above, refers to texture synthesis from a sample (not "procedural" texture synthesis).

2. Plausible restoration, above, refers to techniques for noise removal, image interpolation, and image in-painting. It also has some relevance to lossy image compression, in that decompressing a lossily compressed image requires a plausible guess as to the data that was discarded.

3. Texture transfer, above, refers to a process of giving an image a certain texture copied from another image. For example, a photograph could be given the texture of a painting.

Chapter 2 reviews published literature from this novel viewpoint. Several apparently disparate problems can be seen as instances of the texture operations identified above. In particular, the plausible

---

and readily spotted by eye. Hence the term "plausible restoration" will be used in this dissertation. Another way of looking at this is to say that interpolation picks that "best possible" restoration, whereas plausible restoration randomly samples from the field of possibilities.

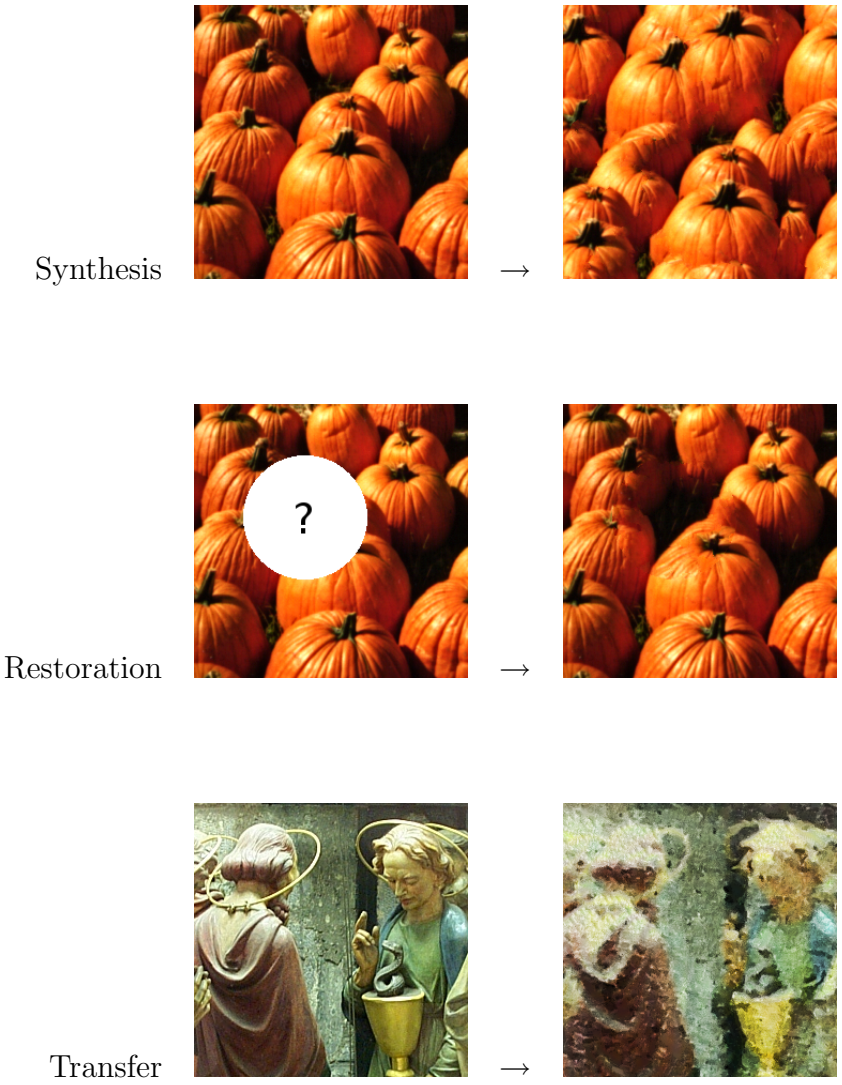

Figure 1.1: Examples of three types of texture operation on digital images.

restoration operation unifies noise removal with interpolation and in-painting of missing areas.

The current state of the art for texture operations on digital images is the "best-fit" method and its variants (see Section 2.2.2). The best-fit method was discovered independently by Garber [1981] and Efros and Leung [1999]. In its most basic mode of operation, when given a sample of texture in the form of an image, the best-fit method can synthesize new samples of that texture. The method may be extended to allow transfer of texture from one image to another, or to plausibly restore a missing area of an image by extending surrounding texture into it.

The texture operations are computationally hard problems. The definition of texture given above allows even for textures that can perform computation such as cellular automata. Sampling from a Markov Random Field is in general an NP-hard problem. In practice, we will see that best-fit synthesis gives rise to types of behavior that, according to Wolfram [2002], are commonly associated with systems capable of computation. Synthesis of reasonable generality and quality most likely requires an algorithm capable of universal computation. This is discussed further in Chapter 7.

The structure of this dissertation is as follows:

Chapter 2 reviews existing literature on image texture operations.

Chapter 3 describes an improvement to the best-fit method. The best-fit method has some fundamental problems, which may be reduced though not removed entirely. Applications to texture synthesis, texture transfer, and plausible restoration of missing areas are described.

Chapter 4 describes enhancements to existing tools for editing and manipulating images. Existing image manipulation software such as "The GIMP" and "Photoshop" have only simple tools for operating on

texture. In images such as line drawings and diagrams, where the texture is simple, these tools are adequate. In photographs, or other images with complex texture, even simple operations require time and skill to produce a good result. The tool described in this chapter makes some of these operations easy.

Chapter 5 describes a simpler method of texture synthesis that in some cases produces results as good as the best-fit method, with less computation. Its application to texture transfer is also described.

In Chapter 6 it is shown that texture modelling allows the removal of various kinds of noise, including compression artifacts, from images. A method is described for plausibly restoring an image in which each pixel value has some specified degree of uncertainty. It is capable of both noise removal and interpolation of a missing region, problems usually considered separate.

Chapter 7 examines some computational aspects of texture synthesis in the context of the arrangement of shaped tiles, placing certain issues that arise in preceding chapters into a broader context. The patterns a given set of tiles may be arranged into are unpredictable and often surprising.

Texture operations on images sit half-way between the fields of Image Processing and Computer Generated Imagery, and cannot properly be described as fully belonging to either field. Texture synthesis from a sample generally requires both modelling and generation of texture. Texture transfer may be seen as filtering by example, or as a way of generating new artistic images. Plausible restoration may be seen as interpolation, but it may also generate new details. Let us begin by reviewing relevant literature from both of these fields.

Chapter 2

Literature review

This chapter reviews published literature relating to how people perceive texture, and how texture may be synthesized, transferred, or used to restore images.

2.1 Perception of texture

The three images in Figure 2.1 are 8, 64 and 256 colour versions of the same scene. There is a clear difference between the 8 and 64 colour versions, but not between the 64 and 256 colour versions, yet all three have an easily measured difference in texture, namely the number of distinct colours.

(a)  (b)  (c) 

Figure 2.1: A scene represented using (a) 8 colours, (b) 64 colours and (c) 256 colours.

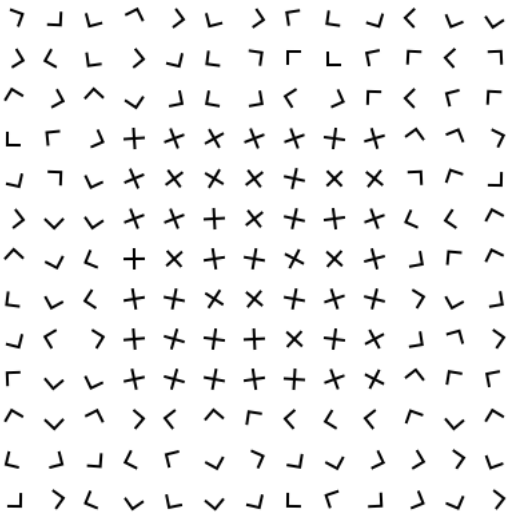

Figure 2.2: Typical figure designed to test texture discrimination [Bergen and Adelson, 1988, Julesz and Kröse, 1988].

What is perceived when people look at texture? We do not note every scratch and mark on every surface, if we did so we would be quickly overwhelmed. Yet neither are we completely blind to these details. While not consciously perceiving details, we do perceive what kind of details there are. What form do these perceptions take?

To determine the aspects of a texture that are perceived, one can test what textures people can discriminate between. A common method is to present people with a figure consisting of several different textures, and ask them to locate the boundaries. A figure typical of the kind used in this type of research is shown in Figure 2.2 [Bergen and Adelson, 1988, Julesz and Kröse, 1988].

The boundary between the crosses and L's in Figure 2.2 is immediately apparent, it "jumps out at you". This occurs in some texture discrimination tasks, while others require closer inspection. Texture discrimination therefore appears to have two distinct modes [Julesz and Kröse, 1988, Bergen and Adelson, 1988]. The first is a fast unconscious mode, called "pre-attentive" texture discrimination. It can distinguish between many, but not all, textures. The second mode occurs when we

scrutinize an image closely and consciously. This mode can distinguish between many more textures, but takes time and conscious attention.

To study the preattentive mode, Hubel and Wiesel [1962] measured the firing of neurons in a cat's visual cortex. They found "simple" neurons that responded to specific patterns such as lines and edges at a specific point on the retina (presumably to detect structural features), but also "complex" neurons that responded to similar patterns anywhere within a certain region of the retina (thus detecting textural properties). They propose that these two types of neuron form the early stages of processing in the visual cortex.

The patterns detected by these neurons do not seem to be predetermined, but rather form during a "critical period" of development. For example, Blakemore and Cooper [1970] raised kittens that were exposed only to lines of a particular orientation during the critical period. Subsequently the kittens had difficulty perceiving lines of different orientation.

Bergen and Adelson [1988] propose a "feature pyramid" as a model of these pattern detecting neurons. A feature pyramid is a collection of edge and spot detectors of different scales. Feature pyramids build on the idea of "image pyramids". The image pyramid of an image is a sequences of images at different resolutions: the image at full resolution, the image at one half resolution, the image at one quarter resolution, and so on. A feature pyramid is the result of taking an image pyramid and applying several (linear) filters to each image to extract different types of feature, such as vertical or horizontal edges. The pixels in such a pyramid will not map exactly to neurons (which will differ from person to person in any case), but may represent a collection of features similar to those detected by people. An example of the features that can be extracted using a feature pyramid is shown in Figure 2.3.

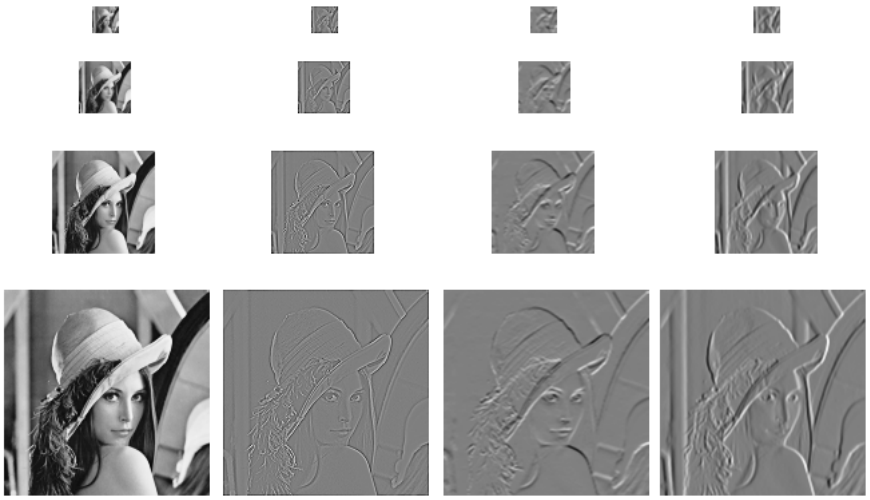

Figure 2.3: Example of an image pyramid (left), and some features that might be extracted from it: spots contrasting with their surroundings, horizontal edges, vertical edges.

However Julesz and Kröse [1988] have shown that feature pyramids are not a perfect model of human perception, by producing a figure in which people could easily discriminate two textures but feature pyramids could not. Julesz suggests that similar figures could be produced for any feature pyramid [Malik and Perona, 1990]. Malik and Perona [1990] note that feature pyramids based on *non-linear* filters can be designed that do not have this limitation.

2.2 Texture synthesis from a sample

This section reviews methods of texture synthesis from a sample. First methods based on the perception of texture are reviewed, then methods based on "Markov Random Fields".

2.2.1 Synthesis via perceptual models

If all perceived properties of a texture are replicated in another image, that image will appear to have the same texture as the original (though it may differ in properties that are not perceived). We might devise some measure we believe to be an objective criterion of how similar two textures are, then design a texture synthesis algorithm that will produce images that exactly match this criterion. This idea has inspired a variety of texture synthesis methods.

Heeger and Bergen [1995] describe a method of texture synthesis based upon the feature pyramid model of Bergen and Adelson [1988], using a "steerable" feature pyramid. A steerable pyramid detects spots and vertical and horizontal edges. The method creates an image having, at each level of the feature pyramid, for each of the three types of feature, the same histogram as that of the sample. The method performs well on simple textures, such as rough stone or wood, but fails to produce a convincing result for textures containing complex features, such as marble or coral, where correlations between features in the pyramid are important.

DeBonet [1997] describes a method that uses a "Laplacian" image pyramid. This type of pyramid has only one kind of feature, spots that contrast with their surroundings. Unlike the method of Heeger and Bergen [1995], DeBonet's method uses correspondences between features, in that the synthesis of features at each level of the pyramid is affected by previously synthesized features at higher levels in the pyramid. It is better able to synthesize complex textures such as coral than the method of Heeger and Bergen [1995]. This is partly because the method reproduces sections of the texture sample verbatim in the output, rather than because the texture is modelled more accurately.

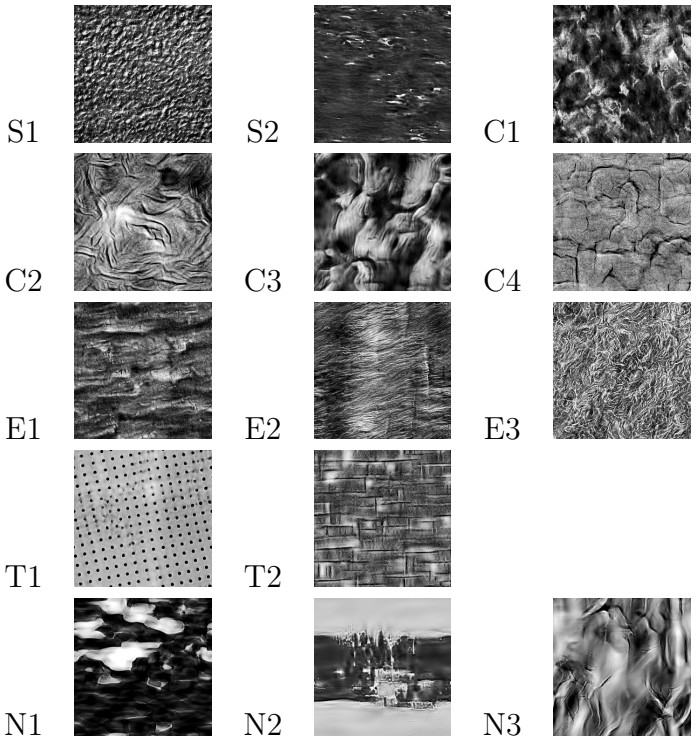

Figure 2.4: Results of applying the synthesis method of Portilla and Simoncelli [1999] to the test suite in Appendix A.1.

Portilla and Simoncelli [1999] describe a method of texture synthesis using complex wavelets. Complex wavelets are a mathematically elegant variety of steerable feature pyramids. The method synthesizes an output which has similar distributions of features and similar co-occurrences of different features to that of the input image. The technique is notable in that it produces reasonable (though not perfect) results on complex textures *without* copying sections of the input image verbatim. Sample results of this method are shown in Figure 2.4.

While these methods are motivated by theories of perception, their results are usually visibly synthetic. This would seem to indicate that our theories of the perception of texture are as yet incomplete. It also implies that objective criteria derived from such theories are not a good way to judge the results of a texture synthesis algorithm: for any criterion we might devise, we can also devise a texture synthesis algorithm that is near-perfect by that criterion but still fails to entirely

fool the human eye. Things are not as bad as they might at first seem, however. At the current level of art, differences between texture synthesis algorithms can be characterized quite easily in qualitative terms and, as people all tend to perceive texture in much the same way (so far as we know), these qualities though difficult to pose mathematically are likely to be consistent between observers.

2.2.2 Synthesis via Markov Random Fields

Pixel inter-relationships in a texture may be treated mathematically as a "Markov Random Field" [Winkler, 1995, pp. 209]. The description of Markov random fields is necessarily abstract, but places many methods described in the literature within a single framework. The reader is encouraged to skim the description below, then read it in detail after looking at the specific applications to texture synthesis given later in this section.

A digital image is a two-dimensional array of pixels. Each pixel has a value (an intensity level if the image is gray-scale, or a vector of colour intensities if it is coloured). If an image is a sample of a particular texture, each possible assignment of values to pixels has a certain probability. A probability distribution may be defined over the space of all possible assignments of values to pixels in an image. This is called a "random field".

A Markov Random Field is a random field with a particular property: Suppose that all but one of the values of an image are known. If the image is a sample from a Markov Random Field, then the likelihood of the unknown pixel having a certain value may be determined solely from the values of a fixed neighbourhood of surrounding pixels. Knowledge of values beyond this neighbourhood provides no further information.

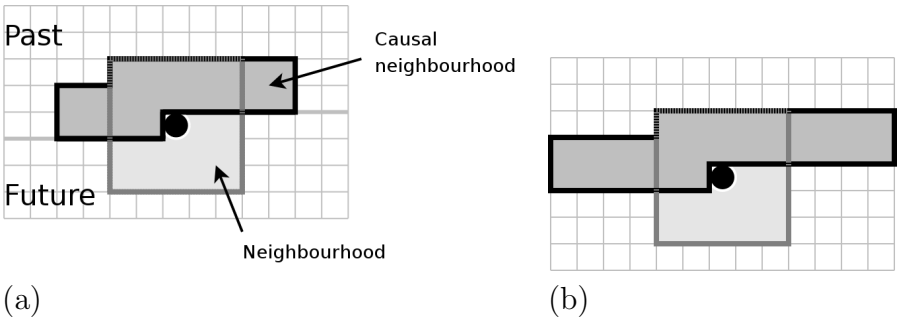

(a) (b)

Figure 2.5: Sequential synthesis: the black dot represents the pixel being chosen. (a) A Markov neighbourhood and a neighbourhood that might be used by a corresponding causal model are shown. The causal neighbourhood includes pixels outside the Markov neighbourhood. (b) In the worst case, the full width of the image might have to be used.

Knowledge of the position of the unknown pixel in the image likewise does not provide further information.

Texture modelling can be seen as the estimation of a Markov Random Field, and texture synthesis as the production of a sample from a Markov Random Field.

As pixel values in a Markov Random Field do not depend on the position in the image, a single sample image is sufficient to estimate a Markov Random Field model. Every pixel and its neighbours is a sample from the conditional probability distribution applying to all pixels of the image.

The method by which a Markov random field is synthesized depends on the form in which it is specified. Some forms afford fast synthesis, while others require lengthy computation.

Suppose the pixels of an image are ordered (for example, in raster-scan order). Further suppose that there is a way to calculate, for each pixel, the probability distribution of possible values given only preceding pixels in the ordering (a "causal" model). Then a sample of the texture may be produced sequentially, one pixel at a time. A random value is chosen for

each pixel, in order, based on the calculation of these probability distributions.

Sequential synthesis is efficient, but has a major drawback: the causal model may need to use the values of pixels outside of the Markov neighbourhood, because a pixel outside the neighbourhood might affect the value of future pixels within the Markov neighbourhood (possibly via several intermediate pixels). The number of pixels the causal model needs to examine could be much larger than the number of pixels in the Markov neighbourhood (see Figure 2.5). The severity of this problem may depend on the ordering of pixels used. For example, rastering from left to right might require a smaller causal neighbourhood than rastering from top to bottom for a particular texture.

If a causal model is not available, or is impractical, it may be necessary to use the Metropolis-Hastings algorithm or one of its variants [Winkler, 1995, pp. 214]. This algorithm produces a sequence of samples which conform to the probability distribution of the Markov random field when produced in sufficient quantity. The algorithm produces each sample in turn by randomly changing one value in the previous sample, then either accepting or rejecting the change. The change is always accepted if the resulting image is more probable than the original, but also sometimes accepted if it is less probable.

The Metropolis-Hastings algorithm requires an initial sample to be chosen, and it may take many many iterations for it to move from the initial sample to a likely sample of the texture.

Texture synthesis methods based on Markov Random Fields will now be described.

Methods with distinct modelling and synthesis stages

Chellappa and Kashyap [1985] describe a way to find an invertible linear filter that produces white noise when applied to a particular sample of texture. That texture can then be synthesized by applying the inverse of the filter to white noise. The filter and a description of the distribution of the white noise values together can be seen as defining a Markov Random Field. The method can reproduce a range of textures, but the simplicity of the texture model limits its ability to reproduce complex textures.

Monne et al. [1981] model texture using a table of the likelihood of each possible assignment of values occurring in a rectangular block of pixels at a random position in a textured image. This may be estimated from a texture sample by counting the number of instances of each possible block of values. The texture sample must be large enough that enough instances of each block are present to yield an accurate probability estimate. The number of estimates required is proportional to the number of distinct colours in the image raised to the power of the number of pixels in a block. This will be large if the number of colours or the size of block is not small, limiting the complexity of textures that may be modelled.

Monne et al. [1981] synthesize images from this model sequentially line by line. For each pixel in each line, information from all pixels in preceding lines is used, as well as preceding pixels in that line (as in Figure 2.5b). The complexity of this calculation rapidly increases with the number of colours and number of pixels in a block. It is only practical with a small block size and a small number of colours.

Best-fit synthesis

The "best-fit" synthesis method has been independently invented at least twice [Efros and Leung, 1999, Garber, 1981]. It is an unusual method in that the new image is synthesized directly from the sample texture, without an intermediating texture model.

Best-fit is a method of causal synthesis, pixel values are chosen one at a time. To choose the value of a pixel, neighbouring values in the output are examined. The sample texture is searched for close matches to this arrangement of values (hence the name "best-fit"). One of the closest matches is chosen, and the corresponding pixel's value is copied to the output image. The goodness of fit of two neighbourhoods is generally defined as the sum of squared differences between them.

Sample results of the best-fit method (using Garber's variant) are shown in Figure 2.6. These results demonstrate both the strengths of the best-fit method and its problems. The method produces plausible variations on the input, to a level of complexity that no other method of texture synthesis can match. However, the results tend to be uneven.[1] Areas of the input may be copied verbatim, especially if there is only one example of a certain feature. Sometimes a pattern will repeat itself inappropriately, producing odd lines or repeating blocks, as can be seen in C1, C3, and E3. Sometimes the algorithm will simply produce garbage, as can be seen in E1 and T1. The texture is also skewed, in a way that depends on the order in which it was synthesized (in the case of Figure 2.6, a top-to-bottom left-to-right raster scan).

The obvious culprit for these problems is best-fit synthesis's causal nature. The neighbourhood of pixels required to accurately synthesize

[1] In defense of Garber, it may be possible to tweak his algorithm to reduce these faults, perhaps by raising or lowering the amount of randomness involved in pixel selection—but it is not easy to predict when or how much tweaking will be necessary.

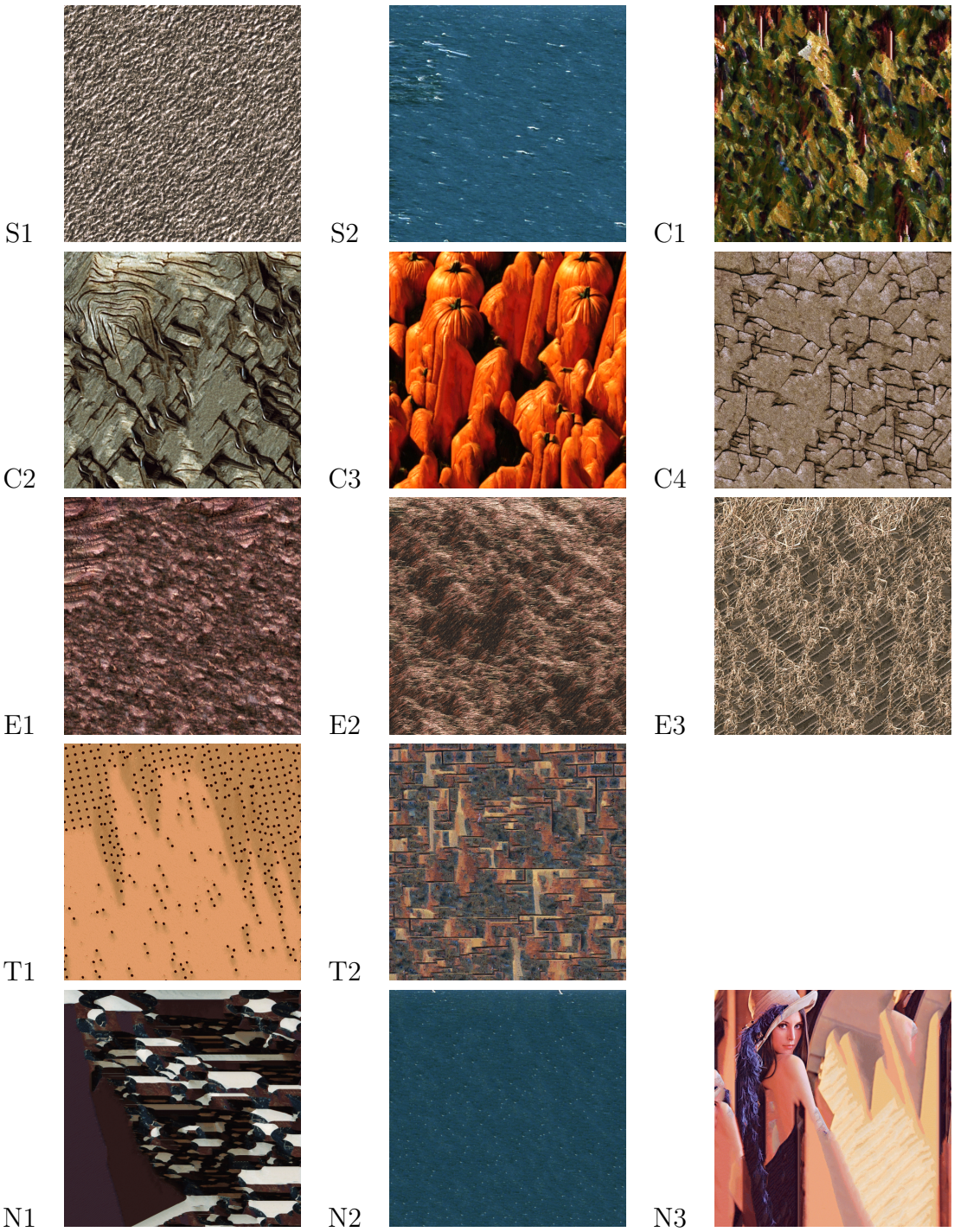

Figure 2.6: Results of applying the best-fit synthesis method of Garber [1981] to the test suite in Appendix A.1.

the texture may be large (as in Figure 2.5), however if the neighbourhood used is large there may be few or no good matches in the texture sample. The result will either be large sections of the texture sample copied verbatim to the output, or garbage [Efros and Leung, 1999]. If on the other hand the neighbourhood used is too small, the output may appear skewed. This effect is especially noticeable if the image is generated in raster scan order. Efros and Leung [1999] make the distortion less visible by adding pixels from the center outwards in an irregular radial pattern. However, it will be seen in Chapters 3 and 7 that this causal nature is not the only source of problems.

The best-fit method is also computationally expensive. For every pixel in the output image, the entire sample texture must be searched for a good match. The high dimensionality of the search space means that even with the use of clever search algorithms, a large proportion of pixels in the image must be considered.[2]

A number of variations on the best-fit technique have been devised that work around the aforementioned drawbacks [Wei and Levoy, 2000, Ashikhmin, 2001, Harrison, 2001, Efros and Freeman, 2001, Liang et al., 2001].

Wei and Levoy [2000] use an image pyramid to reduce the distortion caused by causal synthesis. The use of a pyramid also represents a way to efficiently use a large neighbourhood to select pixel values. Output is generated first at a coarse scale then at progressively finer scales until the desired scale is reached. In other words, an image pyramid is generated from the top down. When choosing each pixel value, causal neighbours on the current level and all neighbours in the next higher

[2]An odd property of high dimensional spaces is that in a cluster of points each point will be roughly the same distance from all other points. This makes it hard to eliminate groups of distant points en-mass using a "kd-tree" search [Friedman, 1977] or similar [Yianilos, 1993, Brin, 1995], as might be possible in 2- or 3-dimensional search problems.

level are examined. As the neighbourhoods examined are partly non-causal, distortion due to sequential synthesis is reduced.

The author [Harrison, 2001] describes a method for ordering the synthesis of pixels so as to minimize the distortion introduced by causal synthesis. This method builds the output a pixel at a time, as in the original best-fit algorithm, but tries at each step to choose a pixel in the output that is highly constrained by the values of its neighbours, and therefore, hopefully, who's causal neighbourhood is not much larger than its full Markov neighbourhood. This serves to hide the "skew" effect, but is otherwise not a large improvement on the original best-fit algorithm. The algorithm is superseded by the best-fit variant described in the next chapter. A copy of the paper has been relegated to Appendix B.

Efros and Freeman [2001] describe a method they call "image quilting" which is significantly faster than the best-fit method. In this, the output is composed of tiles selected from the sample texture. The tiles overlap, and are selected so that where they overlap they are as similar as possible. The texture sample is only searched once per tile rather than once per pixel as in the original best-fit method. A transition line of minimum discrepancy between adjacent tiles is found, in order to disguise tile boundaries. Results are comparable to the best-fit method, except that this method will not produce "garbage". Liang et al. [2001] describe a variety of improvements and optimizations to this method. Kwatra et al. [2003] describe a variant they call "graph-cut" in which the patches can be of any shape. After initial seeding in the manner of Efros and Freeman [2001], the edges of patches are allowed to move about arbitrarily as they search for paths of minimum discrepancy. Graph-cut can also be used as a tool for producing a seamless boundary between two images. Xu et al. [2000] found that results acceptable for some applications may be obtained even if patches are chosen at random, so long as edges are disguised (either by feathering or best-fit synthesis over

the border region). They call this random method a "Chaos Mosaic".

Ashikhmin [2001, 2003] describes an optimization to best-fit synthesis in which only continuations of the areas copied to surrounding pixels, plus a small number of random locations, are considered when choosing each new pixel value. This provides a considerable speed-up, and reduces the "garbage" effect. It can also reduce quality, since the small number of candidates considered for each pixel increases the likelihood of there sometimes being no good match.

2.2.3 Texture synthesis on curved surfaces

In three dimensional computer graphics it is common to want to texture a curved surface, for example to give an animal realistic skin texture. A flat texture may be "mapped" over a curved surface, but this usually distorts the texture—some sections are stretched while others are compressed. To give a surface an undistorted texture, the texture must be synthesized over the surface itself.

If the neighbourhood of a point on a surface can be defined, Markov Random Field models can be adapted to synthesize texture over surfaces. Ma and Gagalowicz [1985] describe a way to do this. On a flat plane, a particular neighbour to a point is a certain distance along a straight line in a certain direction. On a flat plane, direction may be defined in terms of an angle from the up vector (vertical axis). On a curved surface, up and other directions have no clear definition, so a vector field of up vectors must be specified by hand. On a curved surface the equivalent of a straight line is a "geodesic", being the shortest possible path between two points. So, on a surface, a point's local neighbourhood may be specified by stepping along geodesics of set lengths in directions relative to a given vector field over the surface.

Turk [2001] and Wei and Levoy [2001] concurrently developed methods for applying the multi-scale best-fit algorithm of Wei and Levoy [2000] to surface texture synthesis, both with convincing results. Turk's method allows the user to specify direction vectors at a small number of points on the surface, which are then used to produce a vector field covering the whole surface, allowing the user to control the direction of the texture.

Praun et al. [2000] describe a simpler method that involves pasting irregularly shaped patches over the surface until it is covered. This is similar to the Chaos Mosaic method [Xu et al., 2000]. A vector field is again required, to choose the orientation of patches. An interesting finding reported by Praun was that it is better to conform patches to the vector field than to use one point of the vector field to orient a patch and minimize distortion of the patch. By conforming closely to the vector field, stripes of texture curve smoothly rather than bending abruptly at patch boundaries.

2.2.4 Texture transfer

Texture transfer allows one image to be given the texture of another. For example, a photograph could be given a paint texture, producing a synthetic painting. Texture transfer is a natural extension to best-fit synthesis. During synthesis, pixel values are chosen not just to fit well with already chosen values but also to conform to features in the target image.

Texture transfer via best-fit synthesis was invented independently at least three times within a short period by the author [Harrison, 2001], Hertzmann et al. [2001], and Efros and Freeman [2001]. Variants of best-fit synthesis have also been adapted to texture transfer. Hertzmann et al. [2001] have adapted the multi-scale method of Wei and Levoy

[2000], and Efros and Freeman [2001] have adapted their image quilting method.

Texture transfer can be seen as image filtering by analogy [Hertzmann et al., 2001]. Image A is to image B as image C is to what image? For example, texture transfer may be used to sharpen images, given blurred and sharp versions of some sample image [Hertzmann et al., 2001, Ashikhmin, 2003].

2.3 Plausible image restoration

Images may be degraded in various ways. A region of an image may be unavailable (for example, if there is an unwanted object in an image that must be deleted), or the pixel values of an image may be known only imprecisely. A degraded image may be plausibly restored by inventing values for the unknown data that are consistent with what is known.

2.3.1 Restoration from a texture synthesis perspective

Igehy and Pereira [1997] adapted the texture synthesis method of Heeger and Bergen [1995] to the task of plausibly filling in missing areas of an image with homogeneous texture. The texture is matched to the rest of the image through a border area, such that the grain of the image lines up with the grain of the synthesized area. This was applied to removing objects from photographs. For example, an object obscuring a grass background could be replaced by synthesized grass texture. Drawbacks of this method are that it can only be used with simple textures, and that it can not extend features such as edges into the missing region.

Efros and Leung [1999], in their paper describing the best-fit method, also describe filling in missing regions of images. This is trivial for the best-fit method, as it already operates by filling in the image a pixel at a time. Unlike the method of Igehy and Pereira [1997], this can synthesize complex textures and extend features such as edges into the missing region.

As with best-fit texture synthesis, the order in which pixel values are chosen is important. Criminisi et al. [2003] describe a way to choose a good order of synthesis so as to best restore edges. Criminisi et al. [2003] compare their method to the way human visual perception fills in missing edges of partially occluded objects.

Meyer and Tischer [1998] consider an image with randomly corrupted pixels (as opposed to a region of missing pixels). A causal Markov model of the image's texture is required. This model may derived from similar but uncorrupted images. The model used has around 1,000 parameters, and is based on combining the results of several linear predictors. Values for corrupted pixels are then chosen to maximize the likelihood of the image, given the model. An unusual feature of this method is that it is stated in terms of image compression – the most likely selection of pixel values turns out to also be the selection that allows the image to be stored in the smallest number of bits. The method is also capable of identifying which pixels are likely to have been corrupted.

2.3.2 Restoration from a noise removal perspective

The removal of additive noise from an image can be seen as a form of plausible restoration. The addition of noise to an image means that the pixel values are known only imprecisely, and we may then seek plausible

true values of the pixels. Many methods of additive noise removal have been proposed. These methods are of the "interpolation" type (see footnote in Chapter 1) and seek the best possible restoration, even if this best restoration is not representative of the full field of plausible restorations. For example, the restoration will commonly be smoother than is plausible.

Noise removal is a very large field, and this section represents only a sampling of existing work sufficient to convey its character.

One straightforward approach is linear filtering. This method derives from stating that elements in the Fourier transforms of the image (signal) and the uncertainty about the image (noise) will have Gaussian distribution. These elements's variances (the expected "spectral density") are estimated, and from these an optimal "Weiner Smoothing Filter" is derived [Helstrom, 1990]. This filter is always linear. The noise component is commonly taken to be white noise, having a uniform spectral density. The image may be estimated to not contain high frequencies (i.e. to be smooth). Alternatively the spectral density of the image may be estimated from the spectrum of the noisy image. In either case, the resulting Weiner Filter will generally be a low-pass filter.

A low-pass filter will blur any sharp edges in an image, so linear filtering is of limited use for additive noise. The limitations of linear filtering led to investigation of non-linear filters.

Non-linear approaches described in the literature vary in complexity. The Lee Filter [Lee, 1980] is an example of a simple but effective non-linear filter. Where a local estimate of the variance of pixel values is low the filter blurs the image, but where it is high the image is left unchanged. Edges, containing a mixture of two levels and thus having high overall variance, are left un-blurred.

A more sophisticated method based on minimizing the "Total Variation" was developed for the US military [Rudin et al., 1992]. The Total Variation method models the texture of the image as tending to have small gradient at each point. The magnitude of the gradient is assumed to have an exponential distribution. Noise is modelled as being Gaussian. Finding the most likely true image under these assumptions requires minimizing a norm similar to L_1 subject to the constraint that the noise removed has an a priori specified variance.[3]

The texture model of the Total Variation method, by using an L_1-like norm, rates smooth gradients and sharp edges as being equally likely. Consequently, the Total Variation method preserves sharp edges in an image. A texture model that made a more traditional assumption of a Gaussian distribution of gradients would prefer smooth gradients to sharp edges. Rudin et al. [1992] report that the Total Variation method is superior to the human eye at extracting features from a noisy image.

The current state of the art (to the author's knowledge) is a method by Portilla et al. [2003].[4] This is a complex method, but the results justify this complexity. The image first is decomposed into a highly-redundant steerable image pyramid. Elements in this pyramid are then modelled as being linearly related to their neighbouring elements both in value and in level of variance. From this model, the average expected value of each element in the pyramid is computed. An image is then reconstructed

[3]The L_p norm of a list of values x_i is $(\sum_i |x|^p)^{\frac{1}{p}}$. A norm L_p may be mapped by a monotonically decreasing function to a corresponding probability density function of form $ae^{\left(b\sum_i |x|^p\right)}$ (where a and b are constants). For example, L_2 may be mapped to a Gaussian distribution. Minimizing a norm will maximize the corresponding probability density.

[4]Two of the authors of this paper previously published a method of texture synthesis motivated by a model of human vision [Portilla and Simoncelli, 1999]. Their work thus somewhat parallels this thesis in considering texture synthesis and noise removal as related problems. Broadly, the difference in approaches is that they treat texture as being composed of inter-related features whereas this thesis treats texture as the inter-relation of pixels and does not explicitly model features (instead letting features emerge from the rules of pixel relationships).

from this de-noised pyramid.

Specialized methods have also been designed to remove the noise introduced by JPEG compression [Zakhor, 1992, Yang et al., 1993, Llados-Bernaus et al., 1998, Meier, 1999]. JPEG breaks an image into 8×8 pixel blocks and performs a Discrete Cosine Transform on each block. The output of the transform is quantized and stored concisely. When decoding JPEG images, there is uncertainty as to the true value of each element in the block transforms due to quantization. JPEG decoders assume that each element is independent, and for each element minimize the expected error by choosing the center of the range of possible values. This is a reasonable assumption, as the purpose of the DCT is to decorrelate each 8×8 block. However the DCT ignores correlations between adjacent blocks, and the decoder may produce visible block borders if the quantization level is too high.

The method of Llados-Bernaus et al. [1998] is typical of JPEG restoration methods. As in the Total Variation method, this method minimizes a norm subject to constraints. The image is taken to be more likely to be smooth than rough, including across block boundaries. Therefore, differences between neighbouring pixels are expected to be small. Penalties are imposed on each difference by the use of a "Huber function", and these penalties are added to give a measure of how unlikely a particular reconstruction is. Huber functions are a compromise between the L_2 and L_1 norms, combining the smoothness of L_2 with the robustness of L_1. They correspond to a Gaussian distribution of values with fat tails.[5] The pixel values are constrained such that the DCT transform elements, when quantized, match the file being decoded.

Though some of these methods use texture models of moderate complexity, any non-linear components are specified a priori. Adaptation

[5]But see Section 3.1.1.

to the image's texture, though perhaps embedded in a non-linear framework, is limited to linear modelling or the tweaking of a small number of parameters. This limits these methods's ability to restore images with novel features.

New procedures for noise removal are constantly being published. Most of these procedures boil down to ever more elaborate a priori models of image and noise texture (though they are not necessarily described as such). Recent papers have included a procedure that constrains the Total Variation to be below a specified level rather than simply minimizing it as far as possible [Combettes, 2004], a method for enhancing edges while blurring other areas based on diffusion processes [Gilboa et al., 2002], and a denoising technique adapted from fractal image compression [Ghazel et al., 2003] (a potentially interesting approach, however the particular iterated function used introduces block artifacts when used for denoising).

2.3.3 General image restoration

Drori et al. [2003] present an elegant formulation of the plausible restoration problem. The input is an image where each pixel has an alpha value in addition to a colour. Pixels with high alpha are known to high accuracy, while pixels with low alpha are known to low accuracy. The problem is to find an image such that if the input is alpha-composited over it the result has consistent texture. Though not stated in the paper, this formulation encompasses the problem of noise removal if the input image is given a constant alpha value of slightly less than one.

The solution to this problem presented by Drori et al. [2003] is effective but inelegantly complicated, combining smooth interpolation, image

pyramids, and a patch-based variant of the best-fit method. Finding an elegant solution to this elegantly general problem is an open and interesting problem.

Chapter 3

Improving best-fit texture synthesis

In the previous chapter, we saw that the best-fit method can be used to synthesize complex textures, but also that it has some serious problems:

- **Speed:** Production of each pixel in the output requires a full search of the input.
- **Artifacts:** The method sometimes produces "garbage" and repeated patches.
- **Skew:** The order in which pixels are chosen can visibly distort the output.

A long list of attempts to reduce these problems was given in the previous chapter. These involved the used of multi-scalar synthesis, or working with blocks of pixels rather than individual pixels. Use of these techniques places constraints on the size and shape of the image that can be synthesized. These methods may also introduce artifacts of their own. For example, in block based synthesis the seam between blocks can become visible.

10% ... 25% ... 75% ... 100%

Figure 3.1: Pixel values are chosen in random order.

This chapter adds another method to the list.[1] The new method is distinguished, however, by its combination of simplicity, speed, small number of parameters, and the absence of any constraints on the size and shape of the area to be synthesized. It is a practical algorithm and is in current use in the form of an open-source GIMP plug-in (see Chapter 4).

3.1 Algorithm

In this new algorithm, pixel values are chosen one at a time in random order (as illustrated in Figure 3.1). This avoids any possibility of consistent skew due to the order in which pixels are selected. When choosing the value of a pixel, the n nearest pixels that already have values are located.[2] The input image is searched for a good match to the pattern these pixels form (see next section). Once a good match is found, the appropriate pixel value is copied from the input texture to the output. To increase quality, some earlier chosen pixel values are re-chosen after later pixel values have been chosen (see Section 3.1.2).

Early in the process, when the density of chosen pixels is low, pixel values will necessarily be chosen on the basis of far distant pixels. Later, when more of the image has been filled, pixel values are chosen on the

[1] An earlier attempt at addressing some of these problems was presented as a paper at WSCG'01 [Harrison, 2001], a copy of which is given in Appendix B.

[2] Or if there are less than n pixels, however many are available. The first pixel is effectively chosen at random.

basis of close neighbours. This approach is therefore *implicitly* (rather than *explicitly*) multi-scalar.

This implicit multi-scalar approach does not constrain the output to be of a particular set of sizes (as do methods based feature pyramids or tiles), giving it the flexibility needed for practical applications. The lack of constraints is of particular importance when performing plausible restoration of an irregularly shaped area in an image (for example, to remove an unwanted object or blemish).

3.1.1 Searching the input texture

When choosing each pixel value, only a small number of locations in the input texture are examined, yielding a considerable speed-up as compared to a search of the whole image. This optimization was first introduced by Ashikhmin [2001]. The locations examined are:

- Continuations of the regions in the input texture associated with the n nearest pixel values that have already been chosen (i.e. as if the current pixel and one its neighbours formed part of a patch copied exactly from the input texture).
- A further m random locations.

The use of continuations allows production of good results even when a small number of locations are examined in each individual search.

The best fit out of each of these locations is selected, based on comparison of the pattern formed by the n nearest known neighbours of the current pixel to the pattern formed by pixels at corresponding offsets about each candidate location. To make this comparison the algorithm

uses a robust metric[3] based on the Cauchy distribution, as described by [Sebe et al., 2000]. The explanation of this metric first requires discussion of some background assumptions commonly taken for granted:

Each pattern may be represented by a vector u of values $u_1 \dots u_N$, those values being the colour components (red, green, blue) of each pixel in the pattern. Let us model the field of all possible patterns as a mixture of classes (a "mixture model"). We could aggregate sets of similar patterns in the input into similar classes, but this would throw away information about individual patterns, producing poor results (see Wei and Levoy [2000] for example). Instead we shall say that each pattern in the input represents a single class.

Having only one instance u of each class, the best estimate we can make of the center of that class is just that instance u. To fully define each class, we also need a density function giving the spread of possible values v around that center point u, $F(v-u)$. Let us assume that F is the same for each class (having only one instance of each class, we have no information about spread for individual classes). Let us further assume, for simplicity, that each dimension of the spread is independent of each other dimension, and is identically distributed, such that F may be calculated from a single-dimensional spread function f:

$$F(x) = \prod_{i=1}^{N} f(x_i) \tag{3.1}$$

Now, given a pattern v, we can calculate the likelihood of it having occurred if it were it an instance of each of these classes by evaluating $F(v-u)$. If we say that each class is equally likely to occur, the class producing the greatest $F(v-u)$ will also be the class it is most likely to

[3]The word "metric" is here used to mean simply a standard way of measuring something, and not in the strict mathematical sense of a distance function used to define a metric space.

be an instance of, the "best fit".

To avoid floating-point underflow and in order to simplify calculation somewhat it is better to work with negative logarithms than raw probability densities:

$$-\log F(x) = \sum_{i=1}^{N} -\log f(x_i) \tag{3.2}$$

The class that minimizes $-\log F(v-u)$ is the best fit. All that remains is to choose f.

The standard distribution f used in the best-fit algorithm (and in many other algorithms) is the Gaussian distribution. The Gaussian distribution is:

$$\frac{1}{\sigma\sqrt{2\pi}} e^{\frac{-x^2}{2\sigma^2}} \tag{3.3}$$

The negative logarithm of this distribution is proportional to x^2. This is the derivation of the commonly used "sum of squares" criterion, also called the Euclidean distance metric or L_2. Note that the same class will be judged most likely regardless of σ.

The Cauchy distribution, used in the present algorithm, is:

$$\frac{1}{\pi\sigma\left(1+\frac{x^2}{\sigma^2}\right)} \tag{3.4}$$

where σ is the "dispersion", analogous to the standard deviation of the Gaussian distribution.[4] See Figure 3.2 for a comparison of this distribution to the Gaussian distribution. This distribution has very

[4]The Cauchy distribution does not have a finite standard deviation.

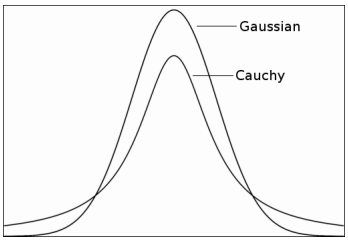

Figure 3.2: The Gaussian and Cauchy distributions.

much fatter tails than the Gaussian distribution, making it robust to outliers. The negative logarithm of this distribution is proportional to:

$$\log\left(1+\frac{x^2}{\sigma^2}\right) \tag{3.5}$$

A sum of these terms is used as the goodness-of-fit metric in the present algorithm, with one term for each colour component (red, green, blue) of each pixel compared. σ is significant for this distribution, and must be specified as a parameter.[5]

If a Cauchy based metric is used, one or two bad pixels in an otherwise good match will not cause that match to be rejected outright, as they would were the Gaussian based metric used. This means that in every search there will be more matches of comparable merit. Repetition and "garbage" are reduced, and overall quality is increased. This is illustrated in Figure 3.4.[6]

[5]So long as we are only concerned with finding the most likely match, not relative likelihoods, the Euclidean distance metric may be simulated in this metric by choosing a very large σ. Indeed, any member of the "t" family of distributions may be so simulated.

[6]The predecessor of this current algorithm, described in Harrison [2001], used the absolute value metric (aka Manhattan distance or L_1). This is another robust metric, and derives from the Laplace distribution ($e^{-|x|}$). This too is more robust than the Gaussian derived metric, increasing only linearly with the degree of discrepancy, but is not nearly as robust as the Cauchy derived metric, which increases as the log of the discrepancy. Another reason to favour the Cauchy distribution over the Laplace distribution is that, as with the Gaussian distribution, it is a member of the Lévy alpha-stable family of distributions (see Mandelbrot [1983, pp.368]). These distributions are produced, amongst other things, in "Lévy flights", a form of random walk commonly seen in nature (and even stock-market fluctuations [Mandelbrot, 1983, pp.337–340]). Processes that give rise to interesting texture, such as textures with a fractal character,

3.1.2 Refining early-chosen pixel values

Early-chosen pixel values are chosen on the basis of far-distant pixels, and may turn out to be inappropriate once nearer pixels have been filled in. Early chosen pixel values are also not chosen with the benefit of being able to continue the regions in the input texture associated with well chosen nearby pixels. For these reasons, the algorithm re-chooses early chosen pixel values once later pixel values have been chosen.

The sequence of choosing and re-choosing used (where N is the number of pixels in the output, and p is some constant $0 \leq p < 1$) is this:

> Choose the first pixel.
>
> ...
>
> Choose the first $\lfloor p^3 N \rfloor$ pixels.
>
> Choose the first $\lfloor p^2 N \rfloor$ pixels.
>
> Choose the first $\lfloor pN \rfloor$ pixels.
>
> Choose all N pixels.

This sequence allows refinement both in the coarse early stages and the fine later stages. It makes good use of the ability of well fitting regions to propagate between neighbouring pixels. The cost of re-choosing can be offset by examining less locations within each individual search. Small modifications to the value of p, so long as a corresponding adjustment is made to n, have very little affect. When re-choosing, the result from the earlier search (the pixel's "continuation of itself") is included in the list of locations examined, and therefore not lost. The value of p used to produce the results presented here was 0.75.

---

often involve Lévy flights.

3.2 Results

Figure 3.3 shows the result of applying the method to the test suite of textures given in Appendix A.1. The $n = 30$ nearest pixels, and $m = 80$ further random locations were used in the searches. $\sigma = 30$ was used in the goodness-of-fit metric (the range of each colour component being 0 to 255).

There are some flaws in the images produced. Certain features in C1 have been duplicated in an obvious way. C3 appears normal at first glance, but closer inspection reveals a number of deformed pumpkins (it is hard to imagine an algorithm that would correctly infer from a single image that pumpkins are distinct objects). In C4, the cracks do not all join up as they do in the original. The tiling patterns (T1, T2) did not produce tiled results. However, overall results were quite faithful to the input.

As might be expected, the images that were not homogeneous textures did not produce sensible results (N1, N2, N3).

The effect of changing σ is illustrated in Figure 3.4. Small σ produces a more representative sample of the input texture, but also produces sharp transitions between patches of texture. Large σ (equivalent to using a sum-of-squares metric) produces smooth transitions between patches of texture, but sometimes some features of the texture are over-represented while others are under-represented. This is akin to the "garbage" produced by the standard best-fit algorithm (see Figure 2.6).

Each image took around 20 seconds to produce, using a 3GHz Pentium-4 processor. The algorithmic complexity is linear in the size of the output. Importantly, it is *not* dependant on the size of the input texture, making this a suitable algorithm for large texture images. This speed makes it suitable for interactive use as a smart selection-eraser, useful for

touching up photographs (this will be discussed further in the next chapter). It would not be suitable for real-time applications such as graphics in a computer game. The speed is comparable with that of tile based methods [Efros and Freeman, 2001, Liang et al., 2001], and the graph-cut method [Kwatra et al., 2003]. The original best-fit method [Efros and Leung, 1999, Garber, 1981] is considerably slower, and would take many minutes to a produce an image of the same size as those presented here. Ashikhmin [2001], who uses a similar search strategy, reports a speed considerably faster than that of this method. This is most likely due to use of a smaller neighbourhood of pixels and less searching per pixel. Note also that Ashikhmin [2001]'s method produces visible artifacts due to the raster-scan order in which pixels are chosen.

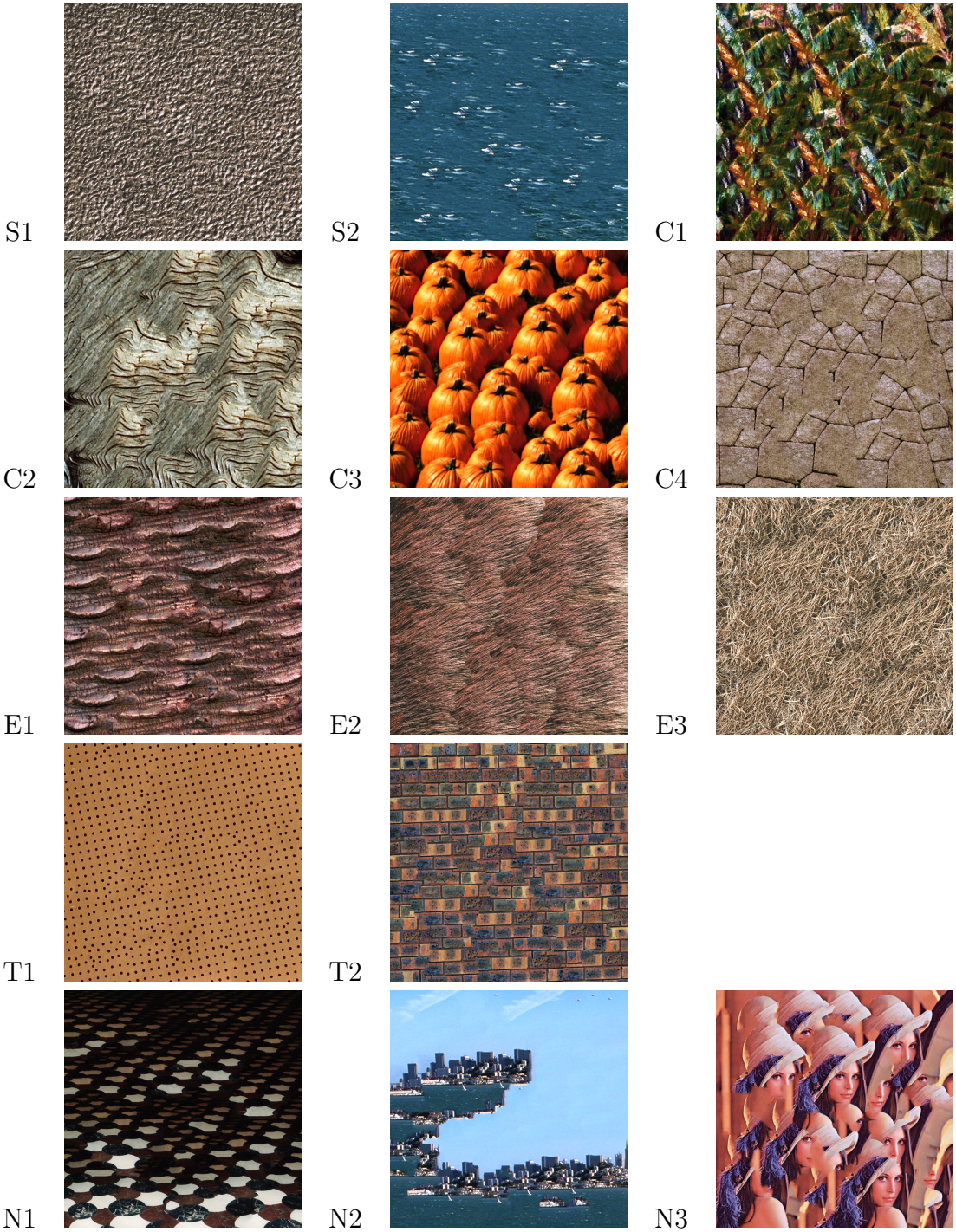

Figure 3.3: Texture synthesis results.

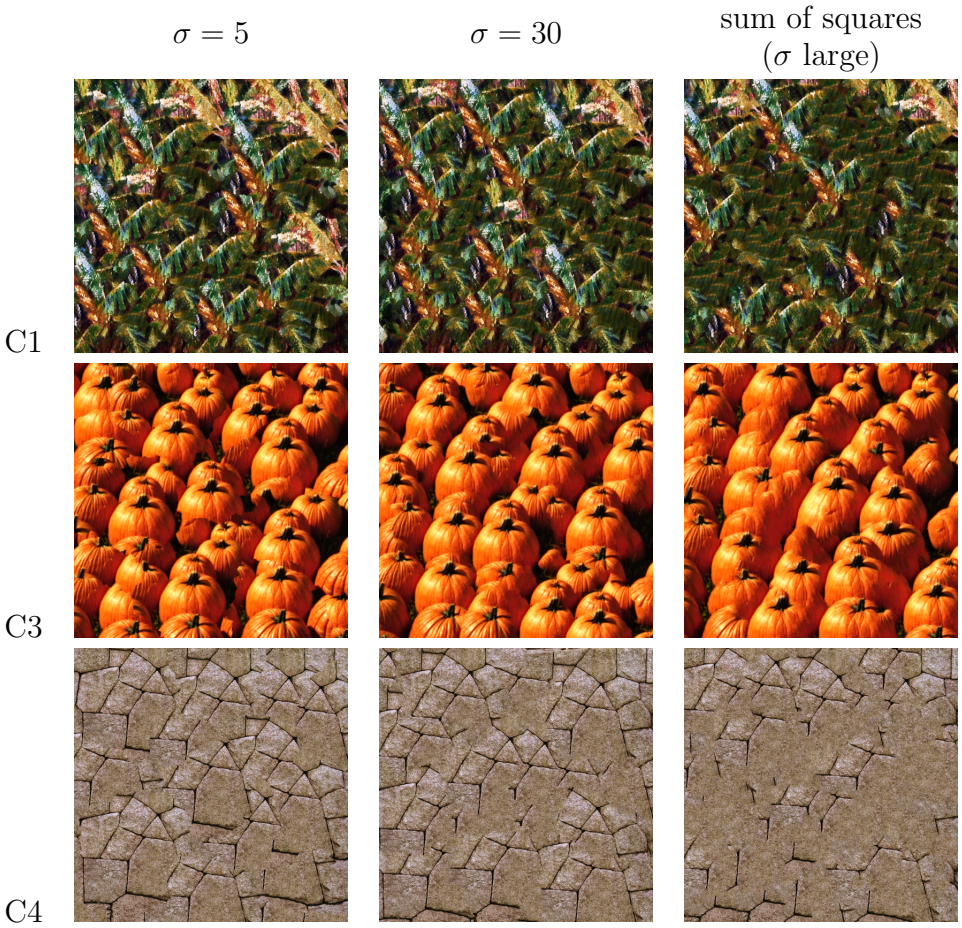

Figure 3.4: Effect of different σ.

3.3 Texture transfer

Texture transfer allows the texture of one image to be transferred to another (see Section 2.2.4). To perform texture transfer, terms may be added to the goodness-of-fit metric in order to specify the layout of different regions of texture in the output image. Two extra images are required, one being a map of regions in the input and the other a corresponding map of regions in the output. In these maps, different colours indicate different regions, and similar colours similar regions. It sometimes suffices simply to use the images themselves as these maps.

In order to retain the multi-scalar nature of the algorithm, it was decided to compare these maps at the same locations as the pixel values being compared, plus the central location. A Gaussian based (squared difference) rather than Cauchy based goodness-of-fit metric was used for these terms, as this was found to give better results. Such a metric heavily penalizes large deviations from the map, while allowing small deviations. This is a good complement to the Cauchy based metric used for the texture itself, which heavily penalizes small magnitude deviations but is proportionately more forgiving of large deviations. The result is an image that replicates the texture accurately in fine detail, but also never deviates excessively from the specified output map.

3.3.1 Results

Texture transfer was applied to the texture transfer test suite given in Appendix A.2, using the texture as its own map. Results are shown in Figure 3.5. Acceptable results were produced from the paint texture (S1), but the jellybean texture (S2) produced less impressive results.

When selecting pixels, the synthesis procedure is searching for

correspondences between a group of pixels in the input and output maps. This search occurs in a space with dimension equal to the number of pixels times the number of colour channels per pixel. To improve results, the size of this search space can be reduced so that there is greater chance of finding correspondences. One simple way to do this is to reduce the maps from colour to gray-scale, dividing the number of dimensions by three. This was used to produce the results shown in Figure 3.6. The input and output maps and the input texture were reduced to gray-scale images. After synthesis, the colour from the original output maps was copied to the synthesized images.

Using this process, the limited palette in the textures is not a problem. The results are now quite faithful to the output map, however some subtleties of colouration present in the textures have been lost.

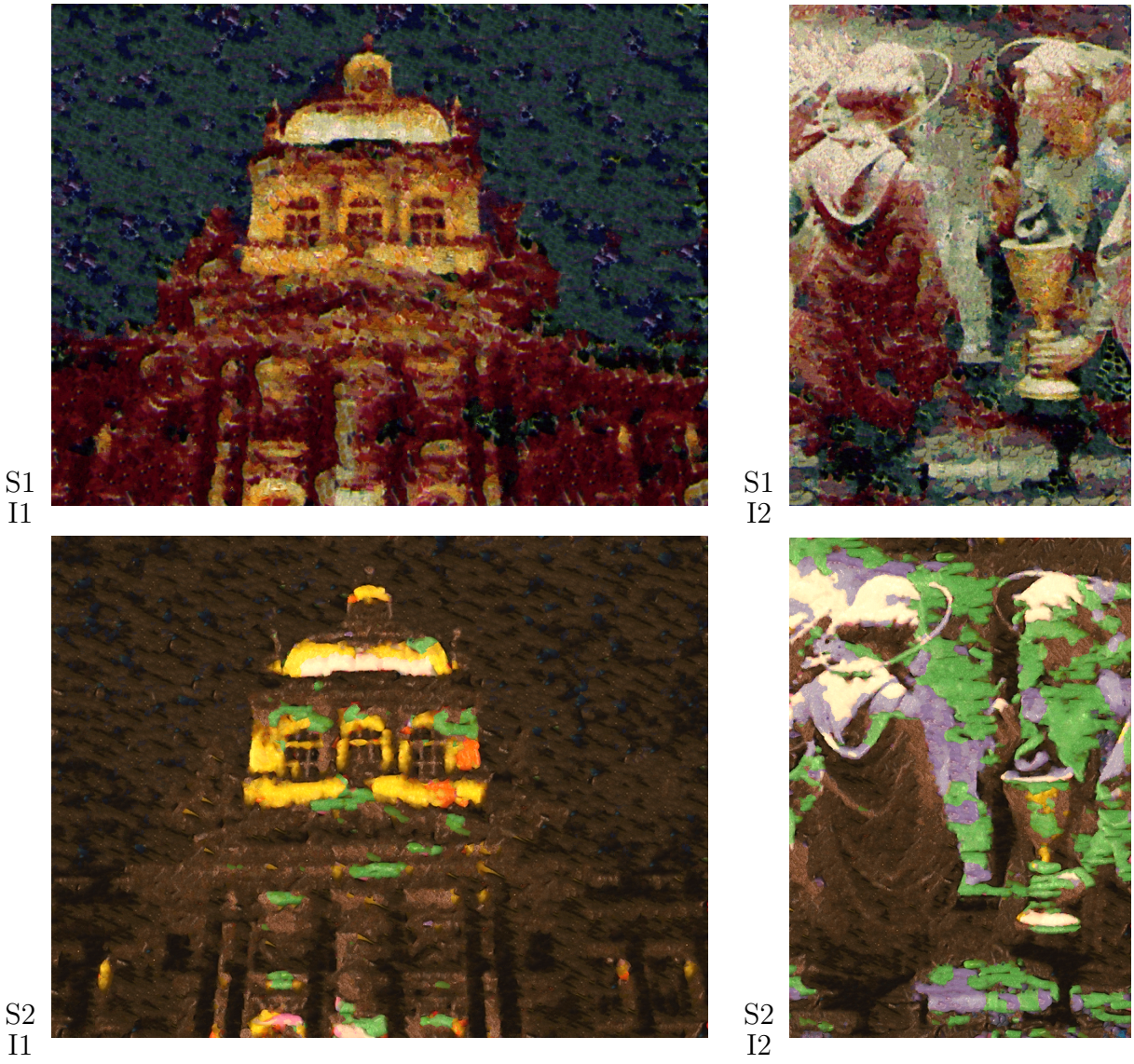

Figure 3.5: Results of texture transfer.

Figure 3.6: Results of texture transfer, retaining original colours.

3.4 Plausible restoration

Texture synthesis has been previously applied to the removal of objects on a homogeneous background by synthesizing a new section of that background [Igehy and Pereira, 1997]. An example of this is shown in Figure 3.7c. Texture transfer allows synthesis of a new background to replace an object, even if the background is non-homogeneous.

Figure 3.7a shows a picture of a donkey standing in a field. In this picture, the field is not homogeneous because of perspective distortion. A feature map of the image (Figure 3.7b) was constructed manually, with parts of the image equidistant from the camera having the same value. The texture transfer variant just described was then used to synthesize a new section of the background to replace the donkey, using the rest of the background as input texture. The new section matches with the existing background and follows the feature map. The result is shown in Figure 3.7d.

3.5 Discussion

The algorithm described in this chapter used a variety of enhancements to the original best-fit algorithm. Choosing pixel values in random order eliminated the problem of skew. Garbage and repetition were also reduced, but not eliminated entirely. Another way of looking at this is to say that even with random ordering certain parts of a texture were obsessively over-represented in the output. The import of this will be explored further in Chapter 7.

The further change of using a robust Cauchy-based metric was required to yield output that was a representative sample of the input. As this is an unglamorous topic, and easily overlooked, it will be mentioned briefly

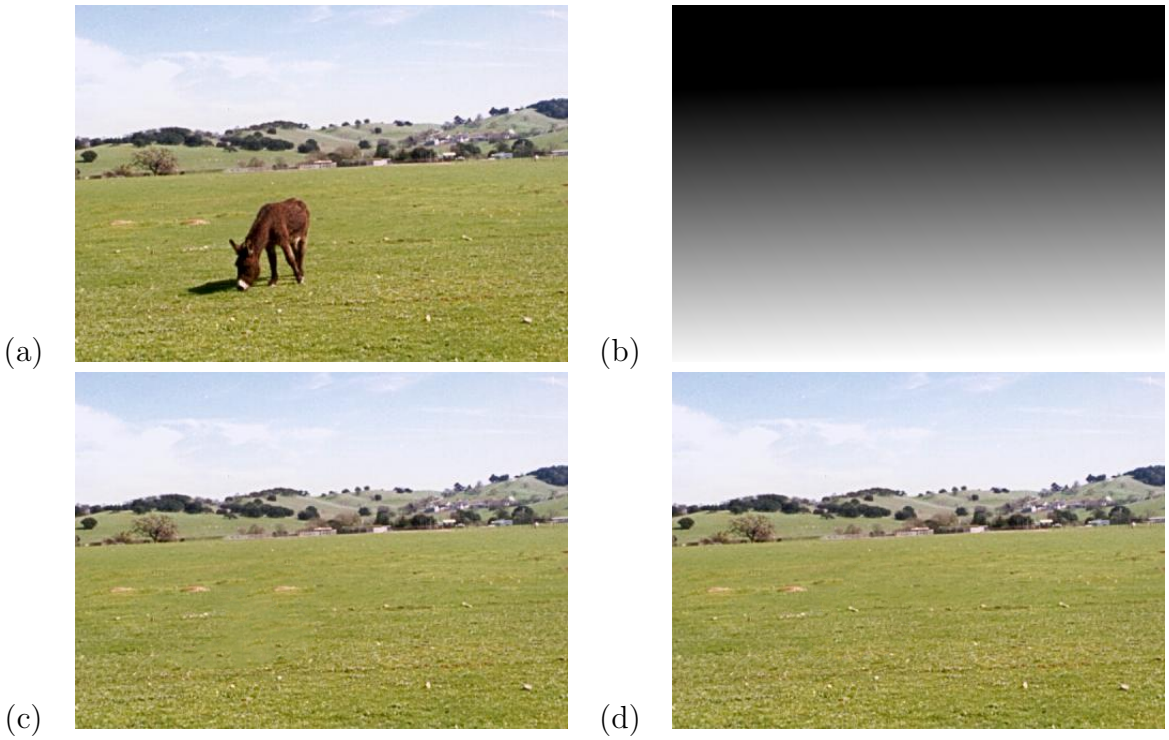

Figure 3.7: Example of object removal. (a) original image (from Igehy and Pereira [1997]), (b) map, (c) object removed without using map, (d) object removed using map.

here that the use of the Cauchy distribution and other alpha-stable distributions in places where the Gaussian distribution and its associated least-squares criterion have formerly been used has yielded improvements in robustness and performance to a wide range of signal processing tasks [Nikias and Shao, 1995]. An ongoing shift away from use of the Gaussian distribution may reasonably be expected in a variety of fields.

The next chapter describes software that allows the algorithm described in this chapter to be used in everyday image manipulation tasks.

Chapter 4

Adding best-fit texture synthesis to the GIMP

In order to be useful, texture manipulation techniques need to integrate with existing software. This chapter describes integration of the method of the previous chapter into the GNU Image Manipulation Program (GIMP, `http://www.gimp.org/`).

The GIMP was chosen because it is popular, and because it provides facilities for extending its capabilities. The GIMP's extensibility comes in two forms, plug-ins and scripts. Plug-ins are written in C or C++, and have low level access to image data structures. Scripts are written in Scheme, Perl, or Python, and can be used to combine plug-ins and the GIMP's built-in tools to perform complex tasks.

The implementation of texture operations may be complex, but the problems they solve are easy to understand. Thus their implementation in software need not be hard to use. Care was taken to eliminate as many parameters as possible. It is impolite to trouble people intent on their task at hand with obscure mathematical details of the tools they use.

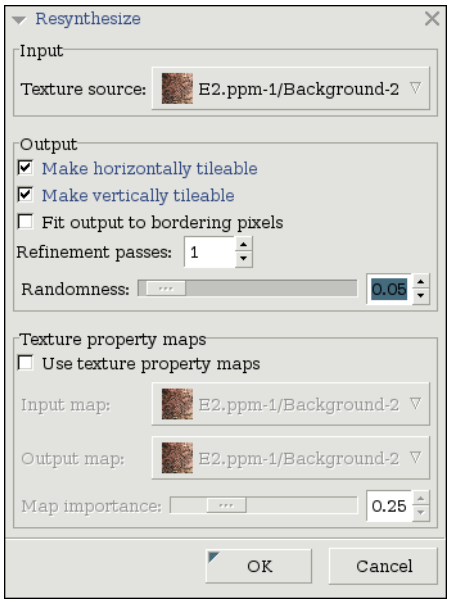

Figure 4.1: The interface to the best-fit synthesis plug-in.

(a)

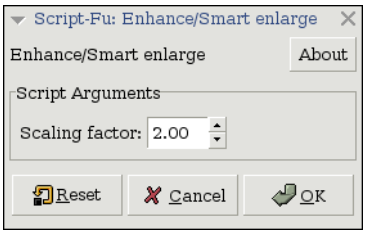

(b)

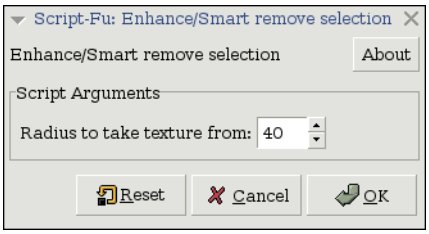

Figure 4.2: Scripts using the best-fit plug-in, which also have simple interfaces: (a) enlarge an image, (b) remove a selection.

A 900 line GIMP plug-in (written in C++) was created to perform the best-fit synthesis variant described in the previous chapter. This plug-in can perform texture synthesis, texture transfer, and plausible restoration of missing areas in an image. It can be obtained from `http://www.logarithmic.net/pfh/thesis` (or the CD accompanying this dissertation).

A screenshot of the plug-in's user interface is shown in Figure 4.1. As can be seen, the interface is straightforward, with a minimum of options.

By using the GIMP's facility for selecting regions, the plug-in can be used to synthesize texture over a specific area of an image. Plausible restoration (as in Figure 3.7) is straightforward.

The GIMP's scripting facility can be used to automate use of the plug-in. For example, a script was written to enlarge images while retaining their texture and the sharpness of their edges (Figure 4.2a). This script works by analogy: an enlarged version of the image is to the image as the image is to a reduced version of the image. Texture transfer is used, where the texture is the input image, the texture map is the input image reduced in size and then restored to its original size (thus losing high frequency components), and the output map is an enlarged version of the input. The script uses a combination of the GIMP's image scaling function and the best-fit plug-in.

A second script was written to delete a selected region by synthesizing surrounding texture on top of it (Figure 4.2b). The input texture is simply a ring of specified thickness about the selection. Figure 4.3 shows an example of this script in use.

4.1 Discussion

There is frequently a gap between the advanced algorithms published in computer graphics journals and the less advanced tools available to non-technical users. The availability of this best-fit implementation has generated considerable interest and positive feedback from users of the GIMP.

Ideally "advanced" tools such as this should disappear into the background, doing their job without making a fuss about their cleverness. The plug-in just described is an everyday tool for everyday tasks.

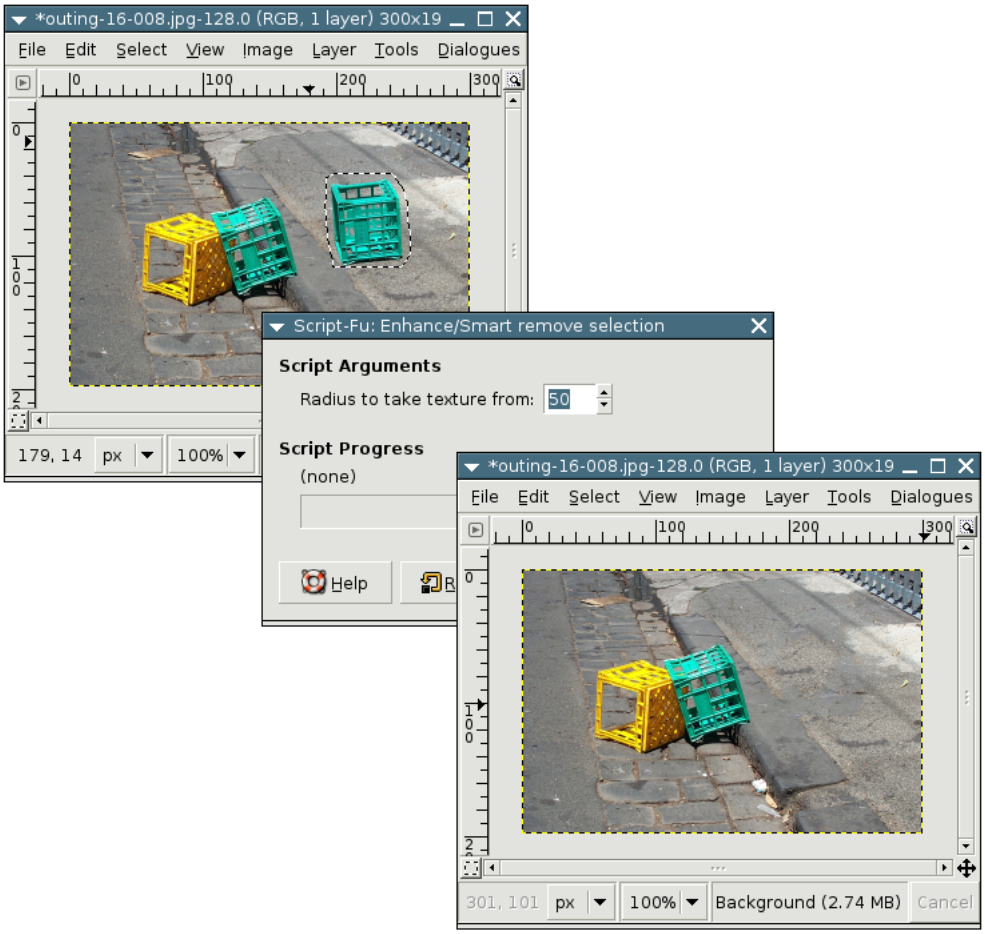

Figure 4.3: Remove-selection script in action.

Chapter 5

Patchwork texture synthesis

Many texture synthesis techniques copy large sections of the sample texture to the output. This can be seen, for example, in the results of the best-fit method (including the variant described in Chapter 3). A number of texture synthesis methods make the copying process explicit. For example, in Efros and Freeman's "Image Quilting" method [Efros and Freeman, 2001, Liang et al., 2001] an overlapping grid of tiles is produced. Each tile is simply copied from the sample texture. Tiles are chosen so that their overlapping regions match as closely as possible.

The Chaos Mosaic method of Xu et al. [2000] takes the idea of copying from the sample texture one step further, with tiles chosen at random from the sample texture randomly pasted onto the output image. No attempt is made to match tiles to each other. Feathering is used to try to disguise tile borders. However, as shall be shown in this chapter, feathering produces visible artifacts.

This chapter examines whether copying random sections of a sample texture is all that is necessary for texture synthesis. A simple method of texture synthesis is proposed, based on random copying. The texture synthesis method is applied to images and to video. Its extension to

texture transfer is also described.

5.1 Method

The texture synthesis method presented in this chapter simply copies random patches of the input to the output, so that the output is completely covered. The edges of these patches are blended together so as to be invisible.

The difficulty lies in making edges within the output invisible. Several types of edges are illustrated in Figure 5.1. As can be seen, a sharp transition (Figure 5.1a) is clearly visible, while a gradual transition (Figure 5.1b) looks duller than the original texture. This kind of transition, sometimes called feathering, was used by Xu et al. [Xu et al., 2000] in their "Chaos Mosaic" texture synthesis method. This dullness can be removed by controlling the standard deviation of pixels in the transition (as described in the next section), producing an invisible join (Figure 5.1c).

An irregular pattern of patches is used, as the human eye is skilled at discerning regular patterns. A Voronoi diagram, based on a set of randomly chosen points, produces a patchwork that is sufficiently irregular.

5.2 Image texture synthesis

In this section, texture synthesis on images is considered. Symbols used in this section are listed in Table 5.1.

First, define the Voronoi cells that are to be used as patches. Choose n

(a)

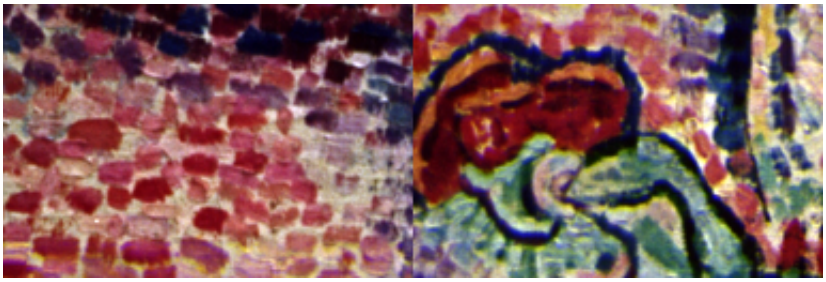

(b)

(c)

Figure 5.1: Joining one texture patch to another by (a) a sharp transition, (b) a gradual transition and (c) a gradual transition controlling for standard deviation.

$O(x)$	Output image
$I(x)$	Input image
p_i	A set of points in the output image
q_i	A set of points in the input image
f	Parameter specifying patch border sharpness
$d(a, b)$	Euclidean distance between points a and b

Table 5.1: List of symbols.

(a) 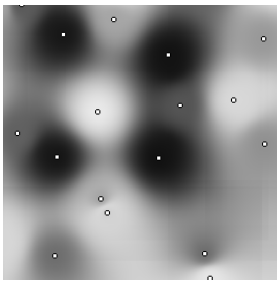 (b) 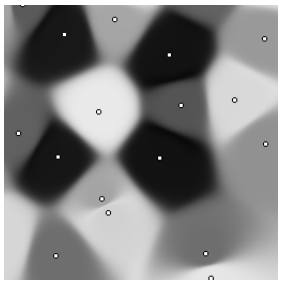 (c) 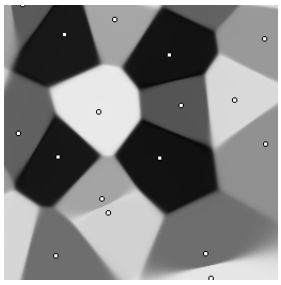

Figure 5.2: Example of patch shapes about the points p_i for (a) $f = 2$, (b) $f = 6$ and (c) $f = 20$

points p_i in the output image $O(x)$. The points p_i form the centers of Voronoi cells, and should be chosen to cover the output evenly. One simple way to achieve this is to choose jittered grid points. The size of the grid determines the approximate size of each cell, as well as the number of points required.

Also choose n points q_i from the input image $I(x)$ at random. These are used to specify the part of the texture sample copied into each patch. The points must be chosen such that for all points x in or near the Voronoi cell of p_i the point $x - p_i + q_i$ lies within the input image. This is necessary to ensure that the portion of the texture sample copied to each patch lies within the texture sample's border.

Let $d((x_1, y_1), (x_2, y_2))$ be the Euclidean distance between two points. Let a be the average colour of the input image. Let f be a parameter defining the sharpness of the edges of the patches (the effect of this parameter is illustrated in Figure 5.2). Assign each Voronoi cell a weight $w_i(x)$ at each point x in the output image

$$w_i(x) = d(x, p_i)^{-f} \tag{5.1}$$

Then the value of each pixel in the output image is calculated using

$$O(x) = \frac{\sum_{i=1}^{n}(I(x - p_i + q_i) - a)w_i(x)}{\sqrt{\sum_{i=1}^{n} w_i(x)^2}} + a \tag{5.2}$$

In this equation, the divisor rescales the result so that its standard deviation is the same as that of the input image. Subtracting out and then adding back the average a ensures that the output image has the same average colour as the input. For efficiency, terms with small weight may be omitted from the summations.

5.2.1 Results

The test suite of images (Figure A.1) was used to test the image synthesis technique. The results of synthesis are shown in Figure 5.3. Many of the synthesized textures (S1, S2, C1, E1, E2, E3) do not contain any obvious artifacts and are not obviously synthetic. However, there is a tendency for large scale structure in the input to be lost, producing somewhat fragmentary or "busy" results. Best results were obtained where the texture did not have large structures, such as objects (C3), cracks (C2, C4), or tiling elements (T1, T2). Random choice of patches is therefore not sufficient for synthesis of all textures, but is practical for a subset of textures.

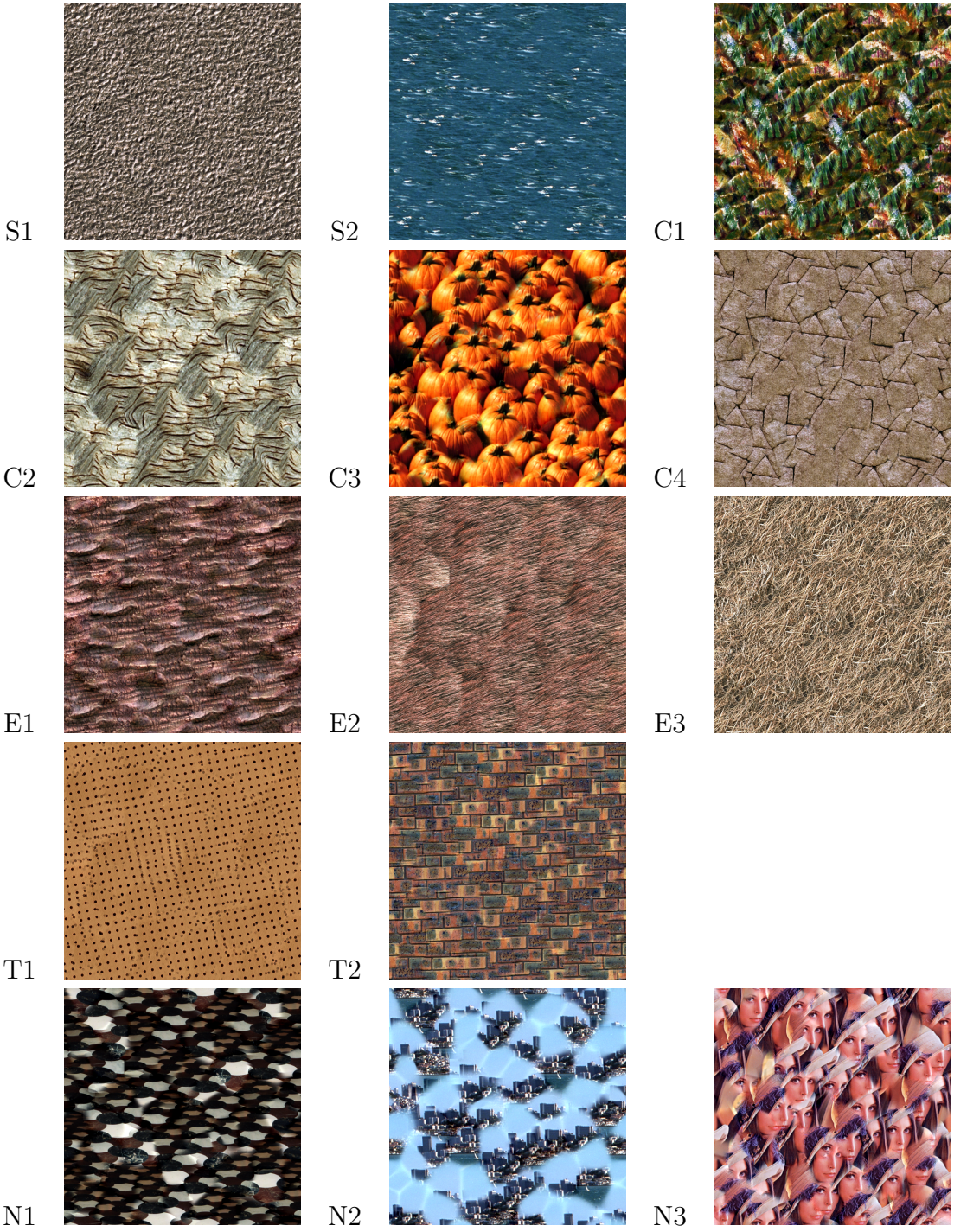

Figure 5.3: Results with $f = 6$, and a grid size of 64 pixels.

5.2.2 GIMP integration

The essential part of the method described in this chapter is the disguising of edges by controlling the standard deviation of pixel values. The GIMP, as with most image manipulation programs, uses alpha blending. As discussed earlier, this produces a result with reduced standard deviation. The effect can be removed by slightly altering one of the layers based on the alpha values, as shall now be shown.

Let c_1 and c_2 be the upper and lower layers being blended respectively, α the alpha value, and c_{avg} the average colour of the upper layer. The standard method of alpha blending is

$$c_{out} = c_1\alpha + c_2(1 - \alpha) \tag{5.3}$$

with c_{out} having standard deviation

$$\sigma_{out} = \sigma_{in}\sqrt{\alpha^2 + (1 - \alpha)^2} \tag{5.4}$$

Thus σ_{out} will be less then σ_{in} for α values not equal to zero or one. c_1 can be rescaled by a factor f to counteract this effect. It is required that $\sigma_{out} = \sigma_{in}$, so

$$\sigma_{in} = \sigma_{in}\sqrt{f^2\alpha^2 + (1 - \alpha)^2} \tag{5.5}$$

producing a scaling factor of

$$f = \sqrt{\frac{2}{\alpha} - 1} \tag{5.6}$$

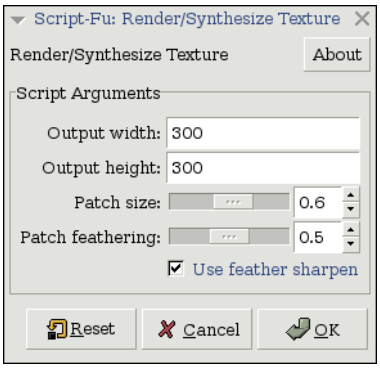

Figure 5.4: Patchwork synthesis script.

The correction is therefore to change the value of c_1 as follows:

$$c_1 \leftarrow f(c_1 - c_{avg}) + c_{avg} \tag{5.7}$$

A 175 line C plug-in was written to provide this. It can be obtained from `http://www.logarithmic.net/pfh/thesis` (or the CD accompanying this dissertation). In combination with the GIMP's built in facility for alpha blending and copying and pasting feathered selections, this provides a method for rearranging parts of an image without modifying its texture.

One problem with this approach is that the colour can be rescaled below zero or above the maximum allowed brightness, and thus need to be clipped. Ideally, clipping would occur after alpha blending. This would require a modification to the GIMP itself, rather than a plug-in.

A simple script was written to synthesize textures by randomly copying and pasting feathered selections from a texture to a new image, making use of the plug-in (Figure 5.4). The results are similar to those seen in Figure 5.3.

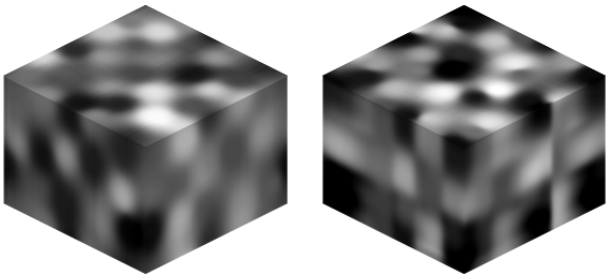

patch-method-1.mpg (a) patch-method-2.mpg (b)

Figure 5.5: Video cubes illustrating the cell shapes of two different video synthesis methods (the vertical axis is time). These videos may be obtained from `http://www.logarithmic.net/pfh/thesis` (or the CD accompanying this dissertation).

5.3 Video texture synthesis

In this section, the texture synthesis method is extended to video. The obvious way to approach video texture synthesis is to treat the temporal dimension as just another spatial dimension, producing a three dimensional mosaic of patches. This is illustrated in Figure 5.5a. It has the drawback that any static elements in the video will become transient in the output. It is therefore proposed to treat the time dimension separately. Patches are fixed between frames, and a separate compositing step is performed in the time dimension, as illustrated in Figure 5.5b. This will preserve any static elements in the texture.

The video texture synthesis method consists of two stages. In the first stage, a set of video sequences are constructed from frames of the input video. In these intermediate sequences, no re-arrangement within each frame takes place, just a re-arrangement of the frames themselves. In the second stage, each frame of the output sequence is constructed from the corresponding frames of the intermediate sequences, using the image synthesis method described earlier in this chapter.

To generate each intermediate sequence, n frames p_i are first chosen in the intermediate sequence, and n corresponding frames q_i are chosen in

the input sequence. The intermediate sequence is generated as a series of transitions between each frame p_i and its successor p_{i+1}.

First, define weights for a smooth transition between p_i and p_{i+1}

$$w_1 = \frac{1}{2} + \frac{1}{2}cos(\pi u) \tag{5.8}$$

$$w_2 = \frac{1}{2} - \frac{1}{2}cos(\pi u) \tag{5.9}$$

where u is the position within the interval $[p_i, p_{i+1}]$

$$u = \frac{t - p_i}{p_{i+1} - p_i} \tag{5.10}$$

Also calculate the average value of each pixel in the input sequence over time, forming an average image $A(x)$. Then the intermediate sequence $N(x,t)$ may be synthesized from the input sequence $I(x,t)$ within the interval using

$$N(x,t) = \frac{w_1 I(x, t - p_i + q_i) + w_2 I(x, t - p_{i+1} + q_{i+1}) - A(x)}{\sqrt{w_1^2 + w_2^2}} + A(x) \tag{5.11}$$

In this equation, each pixel in each intermediate frame is produced by combining pixels from two source sequences. The standard deviation of each pixel is preserved in the result.

Piecing all the intervals together gives a full intermediate sequence.

The output sequence is generated from a set of intermediate sequences. Each frame of the output is constructed by piecing together patches sampled from the corresponding frames of the intermediate sequences as

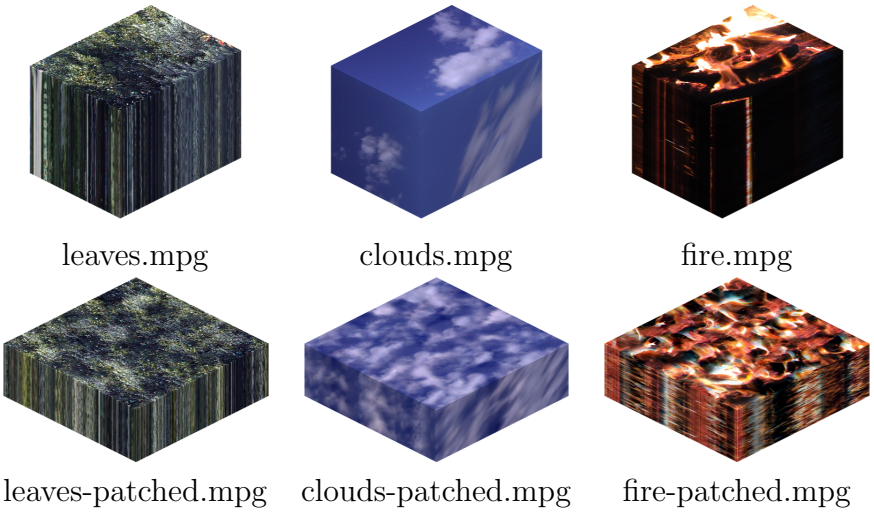

Figure 5.6: Input video cubes (top row) and corresponding synthetic video cubes (bottom row). These videos may be downloaded from `http://www.logarithmic.net/pfh/thesis` (or the CD accompanying this dissertation).

in the image synthesis method. Each intermediate frame contributes one patch to the output frame. Each frame in the output is synthesized using the same arrangement of patches.

For efficiency the two stages of synthesis can be combined, so that the pixel values in the intermediate sequences are only ever calculated as needed.

5.3.1 Results

Results are shown in Figure 5.6. All results are tilable video loops. The first video produced good results. That is, there are no obvious artifacts and the video is not obviously synthetic. The second was less satisfactory, the patches are clearly visible. This is because the movement of the clouds reveals the pattern of patches. The third video also produced reasonable results, although there are some artifacts where bright flame occurred at the edge of a patch.

5.4 Texture transfer

In this section, the texture synthesis method described in the previous sections will be extended to texture transfer. This will first be described in the domain of images, then generalized to video.

To perform texture transfer, two images are required. As before, a texture image is required ($I(x)$). Additionally a pattern image is necessary ($P(x)$). The pattern image defines the pattern of texture desired in the output. For example, by using a painting as the image texture and a photograph as the pattern image a synthetic painting of the photograph could be created.

Patches are again defined in terms of a Voronoi diagram. However, the points q_i in the input texture are no longer chosen randomly. Instead, each is chosen to minimize the sum of squared differences between the patch of the pattern image around p_i and the patch of input texture around q_i.

Finding the exact best match to each patch often means that a particular area of the texture sample is repeated many times in the output. A solution to this problem is to consider only a random subset of points in the image as possibilities for each point q_i. This also yields a substantial speed increase.

The output to be synthesized is no longer homogeneous. The average pixel value varies from place to place. During synthesis this means that rather than using an overall average, a localized average must be used. One way to do this is to calculate an average a_i of each patch. The output can then be calculated from

$$O(x) = \frac{\sum_{i=1}^{n}(I(x - p_i + q_i) - a_i)w_i(x)}{\sqrt{\sum_{i=1}^{n} w_i(x)^2}} + \frac{\sum_{i=1}^{n} a_i w_i(x)}{\sum_{i=1}^{n} w_i(x)} \qquad (5.12)$$

This is very similar to Equation 5.2, the only difference being the calculation of the average.

This transfer technique may also be applied to video. For example, to produce an image with animated texture, the pattern image $P(x)$ might be matched against the average frame $A(x)$. The video texture synthesis method described in section 5.3 can then be applied.

5.4.1 Results

Results are shown in Figure 5.7, based on the texture transfer test-suite (Figure A.2). As a pre-processing step, the pattern images were rescaled so that they had the same average colour and colour range as the texture images. These images took longer to produce than the texture synthesis images, as selecting each patch required searching the texture image.

As with the best-fit method, reducing the dimensionality of the search space can be used to improve results (see Section 3.3.1). The texture and pattern used for texture transfer were reduced to gray-scale images before texture transfer, and the original colour from the pattern image reapplied to the output. This produced the results in Figure 5.8.

An example of video texture transfer is shown in Figure 5.9. The texture used was the video of leaves in Figure 5.6.

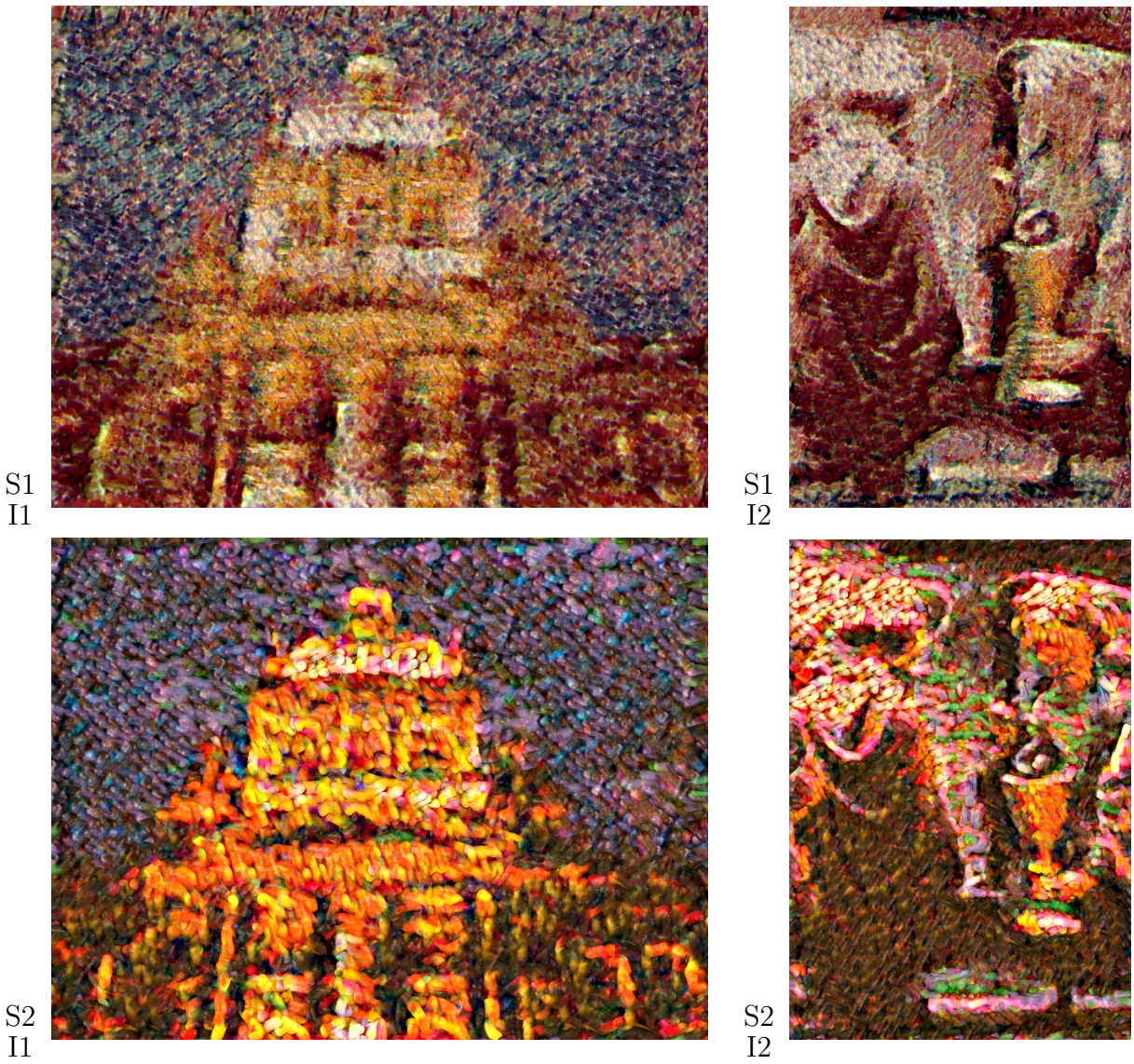

Figure 5.7: Texture transfer with $f = 2$, and a grid size of 16 pixels.

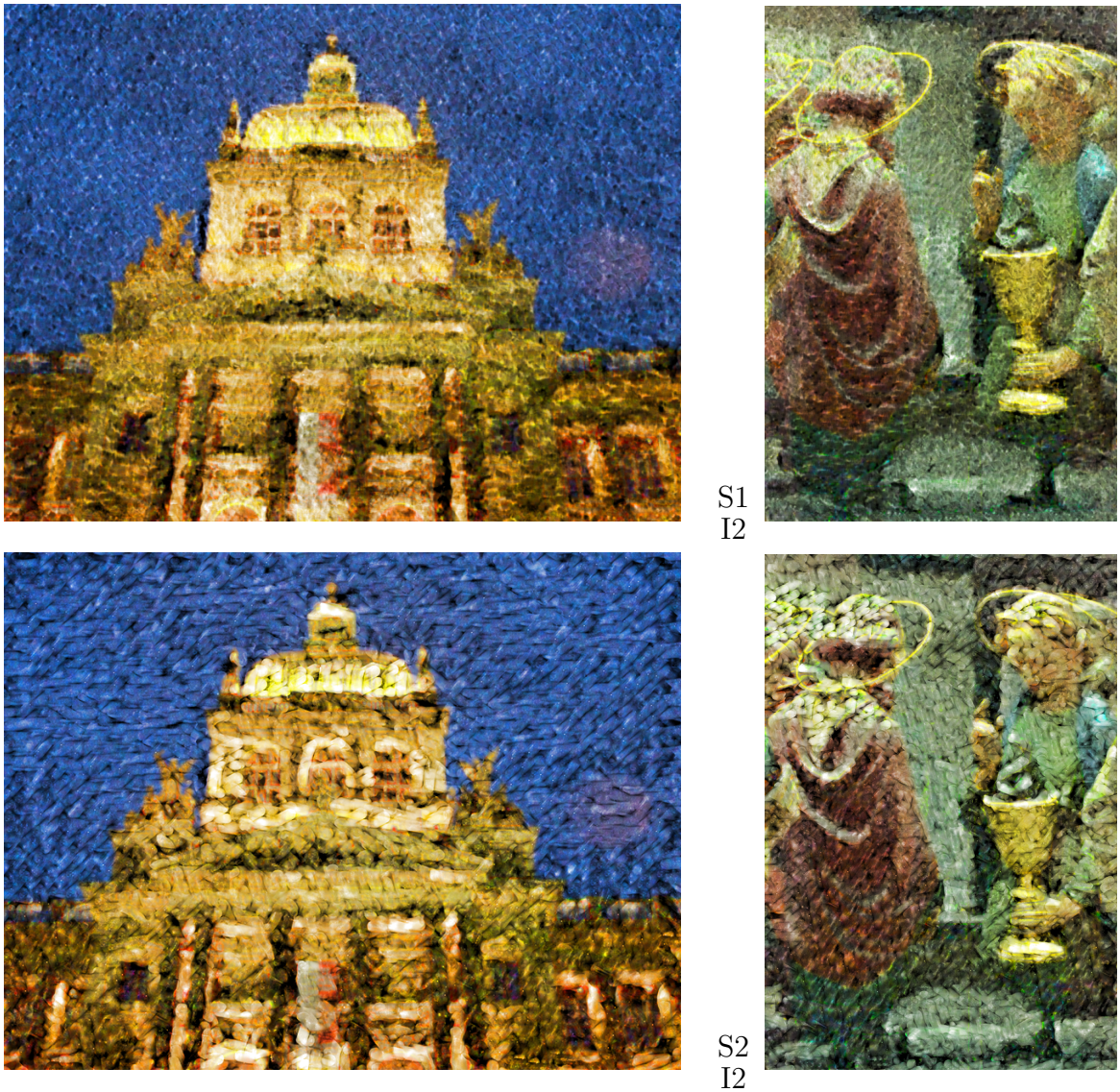

Figure 5.8: Texture transfer with colour copied directly from pattern.

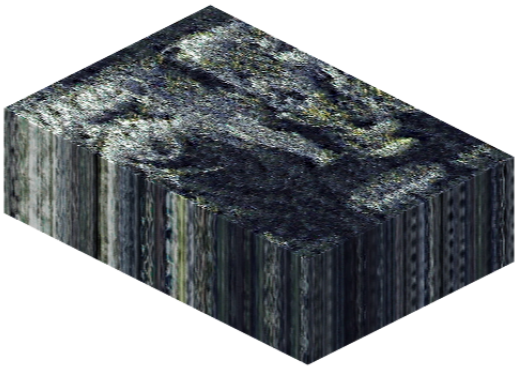

tt.mpg

Figure 5.9: Example of video texture transfer. This video may be downloaded from `http://www.logarithmic.net/pfh/thesis` (or the CD accompanying this dissertation).

5.5 Discussion

The main contribution of this chapter is the method of blending edges invisibly. The texture synthesis technique described in this chapter is simple and fast, and gives good results for many textures.

Would the technique be improved by choosing the patches more carefully, as in image quilting [Efros and Freeman, 2001]? Interestingly, the answer is no. The method used to disguise edges relies on patches being uncorrelated. If patches are chosen so that they are correlated, the edges will be over-emphasized and become visible.

At the start of this chapter it was noted that many texture synthesis methods copy sections of the input, either implicitly or explicitly. If this property is considered separately from the selection of the patches that are copied, their relative importance can be compared. In the technique described in this chapter, the selection of patches was random. Excellent results were obtained with some textures, but others produced poorer results. In particular, tiling patterns and textures with distinct objects produced poor results. It can therefore be concluded that best-fit

selection of patches can only improve textures such as these.

This chapter and the preceding ones have described methods of creating new images with a given texture. The next chapter looks at the restoration of the texture of existing images where that texture has been degraded by noise.

Chapter 6

Plausible restoration of noisy images

The values of pixels in an image may, for various reasons, be known only imprecisely. If so, the texture of that image may be used to help estimate the true pixel values. In a textured image the value of one pixel may give clues as to the values of other pixels. This chapter describes how a texture model may be used to find the most likely pixel values of an image, where only upper and lower bounds on these values are known. A variant that can remove Gaussian noise is also described.

Imprecise knowledge of an image usually takes the form of an image with additive noise. This noise might be generated as a result of storing an image in a lossy format such as JPEG or GIF, introduced while converting it from analogue to digital form, or produced by an analogue device. The amount of noise may depend on the position in the image, or even the content of the image. Restoration of images stored in lossy formats is of particular interest, given the large number of these images that now exist (for example, on the World-Wide Web).

The novel feature introduced in this chapter, as compared to other

methods of noise removal, is the use of complex texture models tailored to each individual image. The kind of textural details seen in an un-degraded part of an image may reasonably be expected to occur in degraded parts. Texture that occurs in the form of large variations may also occur in small details occluded by noise. These ideas can be expressed in terms of texture modelling, allowing more accurate restoration of images.

To attempt removal of additive noise from an image, two things must first be stated:

1. The set of possible values for each pixel, and how likely each of these values is (in other words, the amount and nature of noise).
2. The ways in which pixels may be related to one another (in other words, what kinds of texture the image may have).

Given these two statements, the most likely image and image texture may be found.[1] The way the two statements are made is crucial. They must be precise enough that the result is useful, but must also be stated in a way that affords computation of the result in reasonable time. The difficulty lies in finding a useful trade-off between these two constraints.

As was noted in Section 2.3.2 of the literature review, most methods of noise removal dull the image. The method described here (as with that of Meyer and Tischer [1998]) will not always dull images. While it uses a texture model, it does not require this model to be specified a priori. The method is simple in form, and is applicable to the general problem of additive noise removal.

The method of this chapter uses the following choice of statements:

[1] Most existing noise removal techniques (see Section 2.3.2) can be defined by two statements of this form, though this is often not done explicitly.

1. Each pixel value lies within a specific range, but is equally likely to take any value within that range.

2. The image has texture that may be described in terms of causal prediction.

The next two sections detail and justify this choice.

6.1 Pixel values

Each pixel value is taken to lie within a specific range, but to be equally likely to take any value within that range. This choice does not compete with the texture model to explain small variations, where noise will mean that almost nothing is known anyway. However it totally rules out consideration of large changes to pixel values, so the texture model need not model large changes, such as edges, with total accuracy.

The pixel ranges may be unbounded on one or both sides. For example, a photograph may have been over-exposed when it was taken (the amount of light incident on some areas of the film exceeding the film's range of measurement). Within regions of over-exposure it is known only that the true pixel values exceed a certain amount. There may also be artifacts such as spots obscuring parts of the image. A pixel within this kind of area may be considered to be equally likely to take any value. (This is similar to the technique for erasing objects from images described in Chapter 3. Unlike the technique of Chapter 3 the result may exceed the dynamic range of the input texture sample.)

6.2 The texture model

Given that an image has a certain texture, a texture model specifies the likelihood of each possible assignment of pixel values to that image. Let I be an assignment of pixel values to an image with texture model M. The most likely texture and pixel values are sought, $P(M, I)$ is to be maximized:

$$P(M, I) = P(M)P(I|M) \tag{6.1}$$

If it is assumed each model is equally likely, $P(M)$ is constant and maximizing $P(I|M)$ will maximize $P(M, I)$. This is the well known Maximum Likelihood method [Press et al., 1992, pp. 658].

If an ordering of pixels in the image is chosen (for example, raster scan order), $P(I|M)$ may be written in terms of the conditional probability of each pixel taking a certain value given the preceding pixel values and the texture model:

$$P(I|M) = \prod_i P(\text{pixel}_i|M, \text{pixel}_0, \text{pixel}_1, \cdots, \text{pixel}_{i-1}) \tag{6.2}$$

A way to compute the likelihood of a pixel value given the preceding pixels's values in an ordering therefore constitutes a texture model.

The predicted distribution of pixel values is taken to be Gaussian with constant variance. With this assumption we need only estimate the mean expected value of each pixel, and the Maximum Likelihood method becomes equivalent to the method of Least Squares (the derivation of this equivalence was given in Chapter 3, or see Press et al. [1992, pp. 657–659]). Least Squares requires minimization of the sum of squared differences between a set of predicted and actual values. This sum is

called a "merit function".

The specific predictor used in this chapter is a weighted sum of a set of values computed from neighbours of the pixel that are in its "past", with the pixels being ordered in a raster scan. The values might simply be the values of the pixel's past neighbours (producing a linear predictor). Other values might result from multiplying several values together, or applying some non-linear function to a value, or combining values in some other way. With sufficient values, any function of the anti-causal neighbours may be approximated to arbitrary accuracy with a weighted sum such as this.

Let $V_1(s) \ldots V_n(s)$ be the set of values used for prediction of the pixel $I(s)$, and $w_1 \ldots w_n$ be the corresponding weights. The predictor is:

$$p(s) = w_1 V_1(s) + w_2 V_2(s) \cdots + w_n V_n(s) \tag{6.3}$$

When calculating the values V_n at the edges of the image, the well known reflection technique may be used. If the image is tilable, tiling may be used instead.

The merit function is:

$$\sum_{s \in \Omega_I} (I(s) - p(s))^2 \tag{6.4}$$

The weights of the model w_i and the pixel values $I(s)$ (within the specified bounds) are chosen so as to minimize this merit function.

6.3 Minimization algorithm

The merit function may be minimized numerically. An arbitrary initial image is chosen (within the specified bounds on each pixel), then a two step process is followed: first an optimum model is found given the current image, then an improved image is found given that model. This process is iterated until it converges.

In the first step, the optimum model for the current image may be found precisely. When minimized, the merit function will have zero partial derivative with respect to each model weight. Each partial derivative is a linear function of the model weights. Equating each derivative to zero gives a set of linear equations. These may be solved to find the optimum model.

In the second step the optimum image is approximated numerically, as finding the optimum analytically is difficult. A multigrid method is used, as described in Press et al. [1992, pp. 871–887]. First a scaled down image of the input is optimized, then successively larger versions. At each scale the optimization is performed via gradient descent.

The multigrid method is necessary so that large features can be optimized within a reasonable time. For example, gradients that have been converted to a series of steps by palettization (as in Figure 6.3) would take a long time to optimize at maximum scale.

Three images undergo scaling: an image of the minimum possible values, an image of the maximum possible values, and the current best estimate of the optimum image. The best-estimate image is scaled up by means of bi-linear interpolation, and scaled down by its adjoint operator, as in Press et al. [1992, pp. 875–876]. The minimum and maximum images only ever need to be scaled down, as they are never modified. When scaling down the minimum image, each pixel in the scaled down image

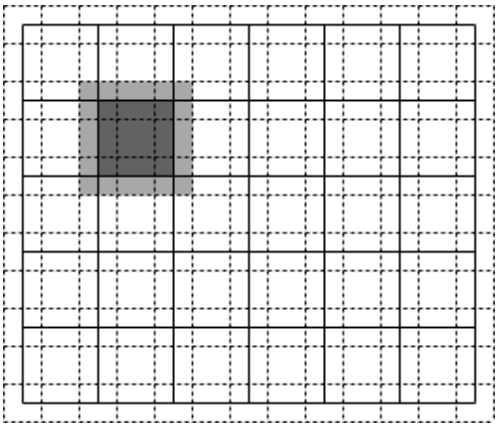

Figure 6.1: Grid positions when scaling an image. A pixel in the coarser grid has been highlighted in dark gray, and the pixels it overlaps in the finer grid highlighted in light gray.

takes the maximum of the nine pixels it overlaps in the original image (as illustrated in Figure 6.1). Similarly each pixel in the scaled down maximum image takes the minimum of the nine pixels it overlaps in the original. Where the value of a scaled down minimum pixel exceeds the value of its corresponding scaled down maximum, both are replaced by the value of the corresponding scaled down best-estimate pixel.

This method of scaling ensures that pixels in the best-estimate image almost never scale up to a value outside of the bounds posed by the minimum and maximum images. While this method is ad-hoc it should not affect the outcome, as the final step is to optimize the image at its original scale.

6.4 Results

The standard "Lena" image [Sjööblom, 1972] was used to test the method. Four different versions of Lena were used:

A. Lena encoded with a palette of only 16 gray levels. The levels were evenly spaced and the image was not dithered.

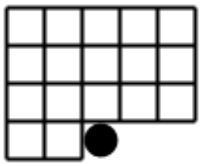

Figure 6.2: Neighbours of a pixel used by the predictor.

B. Lena over-compressed using JPEG, with only 0.385 bits per pixel.

C. Lena with simulated over-exposure. Pixel values exceeding three-quarters of the maximum brightness were clipped.

D. Lena with missing areas.

The texture model used was based on the seventeen neighbours shown in Figure 6.2. The values used by the predictor were: a constant, the value of each neighbour, the result of multiplying the values of each possible pairing of the neighbours (including multiplication of a neighbour by itself), and the result of multiplying the values of each possible triple of neighbours (including cubing of a neighbour, and multiplication of the square of a neighbour by another neighbour). This set of values allows the predictor to take the form of any cubic function of the neighbours's values. The predictor had a total of 1140 terms.

In case A, the true pixel values could vary from those of the image by up to $\frac{1}{32}$ of its total dynamic range. The input and result are shown in Figure 6.3. As can be seen, the distinct levels of the input image have been smoothed into continuous gradients. With the exception of some fine texture in the hat, the detail of the original image has been well preserved. Note, for example, that edges in the image remain sharp.

In case B (Figure 6.4), the distortion is especially visible near the edges of the 8×8 Discrete Cosine Transform blocks used by JPEG. The range of variation was therefore set higher in the edge pixels of each block than

	Input image	Result
A	34.29	**34.92**
B	33.73	**33.15**
C	34.41	**37.39**
D		**29.01**

Table 6.1: PSNR in decibels, as compared to the original Lena image.

the other pixels, and higher still in the corner pixels. Pixels in the corners were allowed to vary by up to 12% of the image's total dynamic range, pixels on the edges were allowed to vary by 8%, and the remaining pixels 4%. In the result, the "blockiness" of the input has been largely removed. Better results could undoubtedly be obtained by more accurately modelling JPEG quantization.

In case C (Figure 6.5), the uncertainty lies in the value of pixels in the over-exposed regions. In these regions the pixels could originally have had any value brighter than their current value. The reconstruction is not perfect, but is a definite improvement on the clipped image. The reconstruction of a fine light edge about the bottom and rear of the hat is a notable success (see the detail image), as is the reconstruction of Lena's left eye.

In case D (Figure 6.6), pixel values in the missing regions may have any value. The overall structure of restored areas is reasonably plausible, but they are implausibly smooth and therefore stand out. It has also failed to extend sharp edges into the restored areas. Also shown in the figure is the result of using the best-fit synthesis technique described in Chapter 3. This highlights the difference between the most likely restoration and a randomly sampled "plausible" restoration. The best-fit method has invented details that are plausible in textural terms, and is also appropriately rough.

Figure 6.3: Input and result for test case A.

The Peak-Signal to Noise Ratio[2] for each case is listed in Table 6.1. Though only an approximation of the perceived image degradation [Bhaskaran and Konstantinides, 1995, pp. 9], the PSNR is a simple and objective measure. The PSNR improved slightly for image A, and substantially for image C. The PSNR of Image B was slightly reduced. A better model of the JPEG quantization algorithm may produce better results.

[2]For 8-bit per pixel images having a noise of standard deviation σ, the PSNR in decibels is $20 \log_{10} \frac{255}{\sigma}$.

Input

Result

detail:

detail:

Figure 6.4: Input and result for test case B.

Figure 6.5: Input and result for test case C.

Input

Result

Best-fit synthesis result

Figure 6.6: Input and result for test case D, and for comparison the result of applying the best-fit technique of Chapter 3.

6.5 A variant for the removal of Gaussian noise

Suppose we have an image with noise added from a uniform Gaussian noise source of known variance.[3] When finding the most likely true image, the variance of the noise at each pixel must be constrained to not exceed the variance of the noise source (the noise in the image is the difference between the true image and the noisy input image).

We can not calculate the variance of noise at a pixel in the image exactly, but we may estimate it from the values of surrounding pixels. To produce this estimate, a convolution of the squared noise image by a Gaussian kernel is performed. This convolved image is then constrained to at no point exceed the variance of the noise source.[4] A kernel of size $\sigma = 8$ was found to give good results.

As in the previous section, gradient descent was used to find the most likely image. The noise within each pixel being independent of surrounding pixels, a multi-scalar method need not be used. After each step of the descent, where the estimated variance of a pixel exceeds the variance of the noise source the pixel value is scaled such that its variance equals that of the noise source.

[3]This is a well studied problem in the field of Image Processing, and applying the algorithm of this chapter to it allows comparison with other noise removal algorithms. However the main intent of this chapter is the framing of a qualitatively different problem, "plausible restoration", rather than further investigation of well studied noise removal problems.

[4]This assertion that the noise is uniform is necessary because the texture model does not take into account that some areas of the image may be more variable than others. A better solution would be to simply constrain the overall variance of the noise, while extending the texture model to include variations in the amount of variation. However, it is not clear how to pose such a texture model in a form that may be optimized within a reasonable time.

6.5.1 Results

The same neighbourhood and predictor terms were used as before. The version of Lena used was the same as that in Portilla et al. [2003] (available from `http://decsai.ugr.es/~javier/denoise`). Portilla et al. [2003] have confirmed that this version is the same as that used in a number of other recent papers. The image is 8-bit per pixel, with 256 possible gray levels.

Results are shown in Figures 6.7 and 6.8. It can be seen that the method has preserved sharp edges well, and has not introduced artifacts into the image, although in Figure 6.8 there are some patches where noise has not been sufficiently removed, giving a blotchy appearance.

The resulting PSNR for various levels of noise is listed in Table 6.2. Results obtained by Portilla et al. [2003]'s steerable pyramid based noise removal algorithm are listed for comparison (this is the best existing Gaussian noise removal algorithm, by this metric, to the author's knowledge). The method described here is not as good as Portilla et al.'s in terms of PSNR. Note however that Portilla et al.'s method introduces some slight ringing-type artifacts[5], whereas the one described here does not. In general, steerable pyramid methods are biassed towards interpreting variations in an image as features from the pyramid, and tend to sometimes infer these features where they are not present.

[5]See `http://decsai.ugr.es/~javier/denoise/examples/simulated_noisy.htm`.

σ	Input image	Result	Portilla et al.
10	28.12	**34.75**	35.61
15	24.61	**32.82**	33.90
20	22.12	**31.31**	32.66
25	20.22	**30.09**	31.69

Table 6.2: PSNR in decibels for the removal of various levels of Gaussian noise. Results obtained by Portilla et al. [2003] are listed for comparison.

Figure 6.7: Input and result for Gaussian noise, $\sigma = 10$.

Input

Result

detail:

detail:

Figure 6.8: Input and result for Gaussian noise, $\sigma = 25$.

6.6 Discussion

The main limitation on the complexity of model used in this chapter was the available computing power. Were unlimited computing power available, a larger neighbourhood and higher-order terms would almost certainly yield further improvement. Every pixel and its causal neighbourhood in an image represents an observation of the image's texture, and an image of (say) 512×512 pixels contains a great many such observations, so a texture model with a great many terms can be supported without danger of over-fitting.

Previous methods of noise removal have adapted their model of texture to images in simple ways, limiting their ability to restore features that are unique to a particular image. The method given here does not have this limitation. Increasing the order of the texture model should allow further improvements.

While it has many more terms than previous models used for additive noise removal, the texture model used here is not fully general. For full generality, the texture model would need to be able to predict arbitrary probability distributions. Specification and optimization of a model this general is difficult. Lesser generalizations are possible, such as prediction of the standard deviation of each pixel in addition to the expected value, or use of robust merit functions based on L_1, Huber functions (as in Rudin et al. [1992] and Llados-Bernaus et al. [1998]), or the Cauchy based metric derived in Chapter 3.

An image restoration technique that can invent details is slightly dangerous. In places where restoration must be reliable, such as medicine or the military, such a method should only be used with care. However, a technique that tailors itself to an image to better restore its specifics may provide enhancements otherwise impossible, which could

be crucial in these places.

If compression artifacts can be removed as they were in this chapter, is lossy compression easy? The standard assumption has been that lossy compression requires a detailed model of human perception, taking into account phenomena such as masking. What if compression artifacts arise simply because the decoder produces images that lack textural self-consistency, and that human perception is sensitive to this? Were decoders to produce more plausible images given limited information, detailed modelling of perception might become unimportant. The lossy aspect of lossy compression might reduce to a simple form of quantization, and the well-studied techniques of lossless compression could be applied. This is, of course, highly speculative.

The method described in this chapter represents a generic method for filling in gaps where a set of data has missing elements or is only known imprecisely. It might, for example, be transferred to the audio domain to reconstruct noisy or clipped recordings, or be applied to other time series data.

Chapter 7

Declarative texture synthesis

Previous chapters have examined texture operations based on synthesizing texture *given a sample*. This chapter looks at how an interesting class of textures may be *designed* using rules specifying which elements in a pattern may be adjacent to one another. This is a slight detour from the main thrust of this dissertation, which is concerned with texture operations that model texture based on a sample of that texture, but serves to place certain curious features of the best-fit synthesis method in a wider context.

The approach of this chapter is to procedural texture synthesis as declarative programming languages are to procedural programming languages, and might therefore be called "declarative texture synthesis". In a procedural language, one specifies a step-by-step procedure by which some output may be produced. In a declarative language, one specifies a set of rules which constrain the output, and it is possible for there to be multiple outputs. Similarly procedural texture synthesis requires a step-by-step procedure for producing the texture to be specified, whereas "declarative" texture synthesis requires a set of rules that constrain the texture that may be produced.

The specific type of rules considered here are specifications of a set of tiles which are to be assembled into a pattern. Some rules will lead to many possible results, some to just one possible result, and some to none at all. If there are many possible results, one is chosen at random.

How simple can local rules of interactions be made, while still producing interesting large-scale structure? The best-fit synthesis method bears some resemblance to the assembling of a jigsaw puzzle, in that it involves the fitting together of many small patches of pixels. If best-fit synthesis is like a jigsaw puzzle, it is one with many different pieces, and it is not therefore surprising that the results also can be complex. However, it is shown in this chapter that even simple jigsaw pieces can result in surprisingly complex forms.

7.1 Specification of the problem domain

The objective is to find a connected structure composed only of pieces from a specified set. Pieces are based on squares or hexagons with edges of various types. An edge of a certain type may only abut edges of some other certain type. Some edges of a piece may be "empty", and these edges do not need to abut another piece. All other edges must abut an appropriate opposite edge. Pieces may be rotated, but not flipped.

There are two possible types of edge:

- Like-compatible edges. These edges must abut another edge of the same type, and will be denoted by numbers (`1`, `2`, `3`, ...). "`-`" shall denote an empty edge, which can also be seen as "like compatible".
- Opposite-compatible edges. These edges must abut some different type of edge, and will be denoted by letters, with each lower case

letter compatible only with its corresponding upper-case (`a`, `A`, `b`, `B`, `c`, `C`, ...).

A piece may be fully specified by a string listing its edges in clockwise order. For example, `--AaAa`.

Were pieces of this type to be used in a physical jigsaw-like puzzle, edges might be shaped as in Figure 7.1. Alternatively, an appropriate arrangement of magnetic or electrical charges on each edge could be used to ensure each edge type connects only to its intended other. If subjected to random impulses of an appropriate magnitude such pieces would, eventually, self-assemble. This would be interesting to attempt at a molecular scale (see also Wolfram [2002, pp. 1193]).

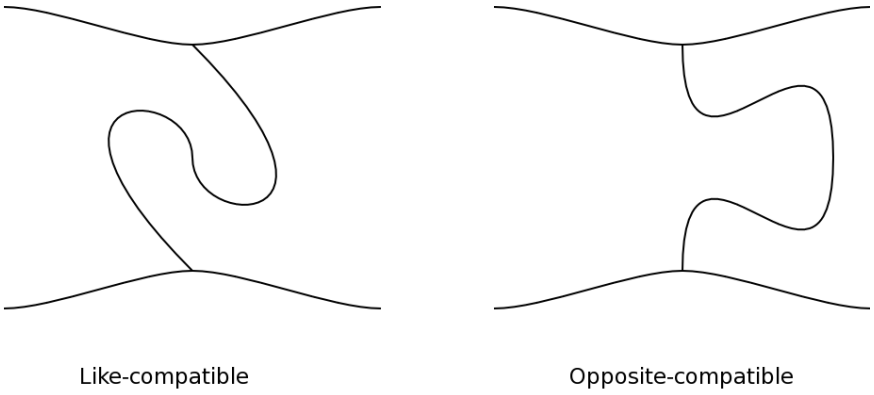

Figure 7.1: The two types of edge, as jigsaw-puzzle type joins.

7.1.1 Relation to Markov Random Fields

Arrangement of tiles depends only on local interactions (the edges of tiles must match), and may be used to define a Markov Random Field. The likelihood of a particular tile being placed at a particular location could be set to either zero, if the tile does not match surrounding edges, or one divided by the number of tiles that could potentially be placed at that location. Similarly the likelihood of an assemblage (of some given size)

will be zero if there are edges that do not match, and non-zero otherwise.

7.2 Literature review

This chapter has one foot in the theoretical topic of tiling patterns, and the other in the practical field of procedural texture synthesis. Some surprising results from the field of tiling patterns will first be reviewed. A brief overview of procedural texture synthesis will then be given.

7.2.1 Tiling patterns

Before the invention of the modern techniques of procedural texture synthesis and tiling of images, one of the most common forms of texturing was tiling patterns produced from small sets of tiles. Such patterns were almost universally repeating patterns, though sometimes of great intricacy.

It is now known that there exist tile sets that may be used to cover the plane, but for which there are no arrangements of tiles that form a repeating pattern. This has particularly been studied in the context of "Wang tiles". Wang tiles are much like the tile sets considered in this chapter, but with the additional restrictions that the tiles are square, and may not be rotated.[1] The smallest known set of Wang tiles that force non-repetition was found by Culik [1996], and contains 13 tiles.[2]

[1] Careful choice of edge types allows one to force all tiles to follow a consistent orientation, so this is really a sub-set of the tile sets considered here.

[2] A somewhat pointless application of Wang tiles to texture synthesis was described by Cohen et al. [2003], in which each tile is decorated with an image who's borders match those of the tiles that may abut it. This can be used to generate infinite, non-repeating texture. But so can a smaller set of tiles, so long as the edge constraints allow some randomness in the choice of tiles. It is easy for a tile set to *allow* non-repeating patterns, the difficulty lies only in *forcing* non-repetition.

If rotation and arbitrarily shaped tiles are allowed, tile sets that force non-repetition containing as few as two tiles are known. Penrose's "kites and darts" are a well known example of this [Grünbaum and Shephard, 1987, pp.531]. It may be possible for a single tile to force non-repetitive tiling, but no tile is currently known that has this property.

Once one realizes that non-repetitive tile sets are possible, one quickly also realizes that there are tile set analogues for all kinds of systems. Wang tile sets have been described that find prime numbers, enumerate the Fibonacci sequence, and simulate Turing machines and cellular automata [Grünbaum and Shephard, 1987, pp.604–606]. The ability of Wang tiles to simulate Turing machines shows that assembly of tile sets is a form of universal computation.

We may then ask whether randomly chosen tile sets commonly lead to complex computations, or whether this is simply a pathological case. This is a question not of existence but of likelihood, and requires computational experiments rather than mathematical deduction, a form of investigation championed by Stephen Wolfram [2002]. Much of what Wolfram has to say is relevant to this chapter, so his theories will now be described in some detail.

Wolfram examined the general behavior of many discrete systems using computational experiments, though with a particular focus on "cellular automata", a form of causal Markov Random Field. The sheer breadth of Wolfram's investigations show that his observations have some generality, and we may reasonably expect them to apply to tiling patterns.

Wolfram found that an enumeration of the simplest possible rules for a given class of system will commonly contain systems having surprisingly diverse behaviors. He identifies four basic classes of behavior:

1. Repetitive: The system repeats within a finite time.
2. Nested: The system produces a self-similar fractal pattern.
3. Autoplectic: The system produces pseudo-random output.
4. Complex: The system produces a diversity of behaviors. Particle-like entities called "gliders", with complex interaction rules, often occur in such systems.[3]

Systems with more complex rules chosen at random were also found to display these same classes of behavior. The complexity of the rules of a system appeared to have little effect on the complexity of their behavior.

Wolfram is of the opinion that simple constraint systems rarely produce interesting results. This is certainly true for the particular family of constraint systems he investigated. He also argues that, although constraint systems can be used to describe limiting states of causal processes as time goes to infinity, such causal processes may take an unreasonably long time to find such states, making constraint systems a poor approximation to observed phenomena. For this reason, Wolfram largely restricts himself to the study of causal systems. It is the author's opinion that while this is an important insight, writing off non-causal systems completely is excessive.

7.2.2 Procedural texture synthesis

A common form of procedural texture synthesis is to define a function mapping position to colour values (or sometimes heights on a bump map). Different textures may be produced by different functions. Regularly repeating textures may be produced by sums of sine waves, or

[3] In a cellular automaton, a glider is a pattern that repeats after some number of time steps, offset some number of squares from its original position.

of the position modulo some quantity, or functions thereof. Random textures are commonly built from lattice noise functions. Lattice noise functions interpolate between pseudo-random values (or values and gradients) on a discrete grid, the pseudo-random values being calculated by applying a hash function to their position. Such noise functions may be summed over several scales to produce fractal noise, or may be used to perturb the position parameter given to some other function to mimic turbulence. A wide variety of natural looking textures can be built by these means, including smoke, marble, wood, and, used as a height function, mountainous terrain [Perlin, 1985, Ebert et al., 1994].

Which of Wolfram's classes can be produced in this way (or mimicked sufficiently well to fool the human eye)? Repetitive or nested texture is straightforward to produce. Random textures that mimic autoplectic phenomena are also straightforward to produce using lattice noise functions. However creation of patterns that imitate textures from Wolfram's complex class is not computationally feasible, as these contain long range correlations that are readily discerned visually, and the texture function would need to recompute these correlations for every point.

Such procedural textures are typically thought of as covering the entire plane (or three dimensional space), and any given sample of texture is a section cut or carved from this. There is no easy way to match the details of one texture to another at a boundary. This is a drawback, as textures in nature often merge into one another in interesting ways (for example the boundary of growth of lichen on rock depending on the texture of the rock, or the stem of a plant extending into a leaf in a branching pattern).

More generally, a procedural texture may use some complex pre-calculation before calculating the value of each pixel. Such

generalized procedures *are* able to generate textures belonging to Wolfram's complex class. Examples of such pre-calculations are finding a Voronoi diagram (in order to produce a texture containing cells), or executing some number of iterations of a two dimensional cellular automaton (such as a reaction diffusion system, to produce spots or stripes [Turk, 1991]). They may also be used to produce textures that blend one into the other [Zhang et al., 2003].

7.3 A tile assembler algorithm

Whether a set of tiles can be assembled into a consistent pattern is undecidable, and within a finite area is NP-complete (see Wolfram [2002, pp. 942]). There is therefore no algorithm that can *guarantee* to assemble an arbitrary set of tiles within a reasonable time. However, an algorithm can be devised that handles many common cases.

Assembly only within a finite area is attempted. The definition of the problem allows us to say that tile placements must conform to a regular grid, and only a finite set of locations need be considered. The algorithm is as follows:

1. Place a randomly chosen tile in the center of the grid.
2. Make a list of empty locations in the grid with abutting non-empty edges. If there are no such locations, halt. Otherwise, if there are any sites where only either one or zero types of tile could be added, restrict the list to just these sites. From the list, choose the location closest to the center of the assemblage.
3. If there is no tile that fits at that location, or if it can be determined that for any tile that might be added the assemblage will become non-completable (see next section), perform

backtracking. That is, remove some number of tiles from the assemblage in the reverse order to which they were added (see the section after next).

4. Otherwise choose a tile at random from the remaining possibilities, and put it at the location.

5. Go to step 2.

An implementation of this algorithm is available from `http://www.logarithmic.net/pfh/thesis` (or the CD accompanying this dissertation).

7.3.1 Determining if a partial assemblage cannot be completed

An empty cell will be part of a region of empty cells. Whether such a region can ever be filled is completely determined by the edges abutting it. To make use of this fact, a hash-table is kept of region boundaries known not to be completable. If adding a certain tile will create a region that is in this hash-table, adding that tile will make the assemblage non-completable.

If it is determined that no tile can be added at some location, the region that contains that location is added to the hash-table. This allows progressively larger regions to be added to the hash-table, and also prevents previous failures from being repeated.

7.3.2 How much to backtrack

In step 3, the assembler may need to backtrack by some number of tiles. The problem may be in a tile added quite recently, in which case only a

small amount of backtracking would be necessary, or in a tile added much earlier, in which case a large portion of the assemblage may need to be discarded.

In the absence of any procedure by which to determine a good number of tiles to backtrack, the approach taken here was to backtrack by a random amount. As we do not know even the scale on which to operate, the amount chosen is sampled from a power-law distribution (power-law distributions are scale-invariant). This ensures that if a large backtrack is required the assembler will perform that backtrack within a reasonable time (for example, in less than the lifetime of the universe).

The specific distribution used was:

$$P(n) \propto (n + a)^{-b} \tag{7.1}$$

where n is the number of tiles to remove ($n > 0$, integer), and the parameters a and b define the personality of the assembler. The parameters affect how long the assembler will take to finish, and may also bias the result towards the emergence of one or another kind of feature. The parameter values used in this chapter were $a = 0.35, b = 3$.

7.4 Results

7.4.1 Single-tile patterns

All possible tiles from some simple classes were tried, as shown in Figures 7.2, 7.3, 7.4, and 7.5. Only tiles that could be arranged into a self-consistent pattern are shown. Even with simple tiles, a great variety of forms result.

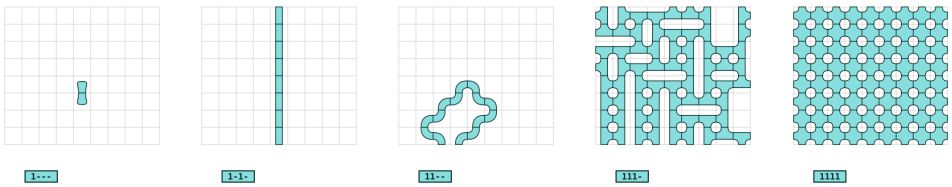

Figure 7.2: Samples of patterns formed by all possible single square tiles having a combination of empty and one type of like-compatible edges.

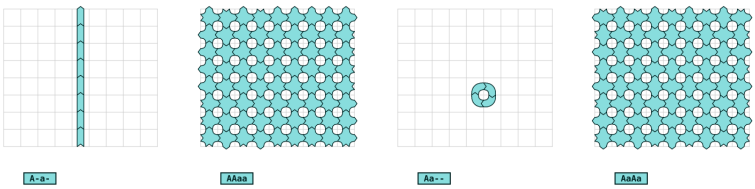

Figure 7.3: Samples of patterns formed by all possible single square tiles having a combination of empty and one type of opposite-compatible edges.

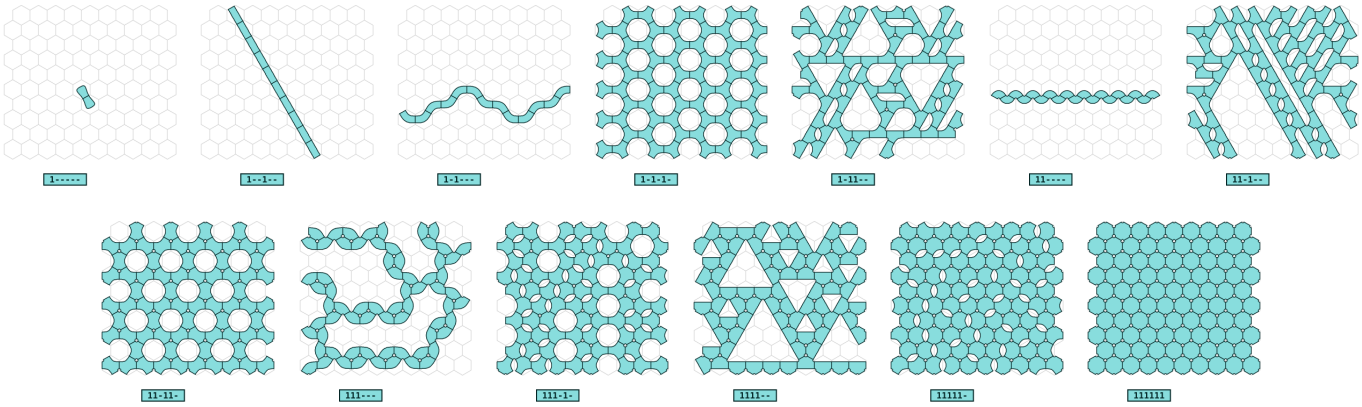

Figure 7.4: Samples of patterns formed by all possible single hexagonal tiles having a combination of empty and one type of like-compatible edges.

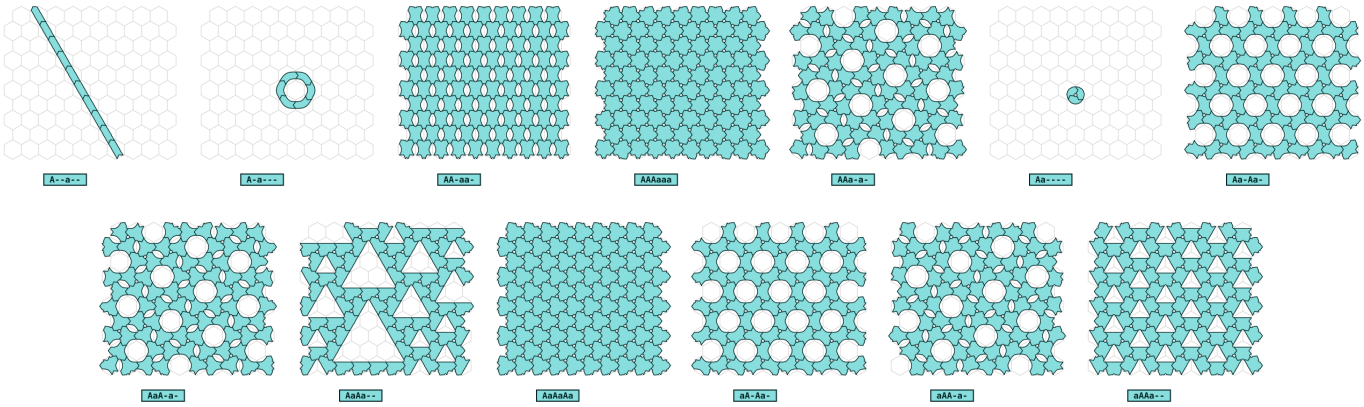

Figure 7.5: Samples of patterns formed by all possible single hexagonal tiles having a combination of empty and one type of opposite-compatible edges.

As might be expected, regular tilings of various kinds can be seen (`1111`, `AAaa`, `AaAa`, `1-1-1-`, `11111`, `AA-aa-`, `AAa-a--`, `Aa-Aa-`, `AaA-a-`, `AaAaAa`, `aAA-a-`, `aAAa--`).

Some tiles form patterns of finite size (`1---`, `Aa--`, `1-----`, `Aa----`, `A-a---`).

`A--a--` and `1--1--` are analogous to simple gliders. If one dimension

were to be arbitrarily interpreted as time, these would appear as a single moving tile.

Various forms of randomness can be seen. This is true randomness, not Wolfram's "autoplectic" pseudo-randomness. `11--`, and `1-1---` follow random paths (which may form closed loops). `111---` forms two kinds of composite units, one with two exposed edges and one with three exposed edges. A random network results, in which the three-edge units are nodes and the two-edge units form random paths between these nodes. `111-` produces rectangles of random size and shape. `1111--` produces triangles of random size and orientation. `AaAa--` produces triangles of random size, but of only one orientation. `AaAa--` turns out to be related to the Sierpinski Triangle fractal, as will be seen in the next section.

7.4.2 Further tile sets of interest

Certain tile sets require a great deal of back-tracking on the part of the assembler. These tile sets are often also visually interesting. Two such sets are shown in Figure 7.6. The set on the left yields patterns with interesting local mirror symmetries.

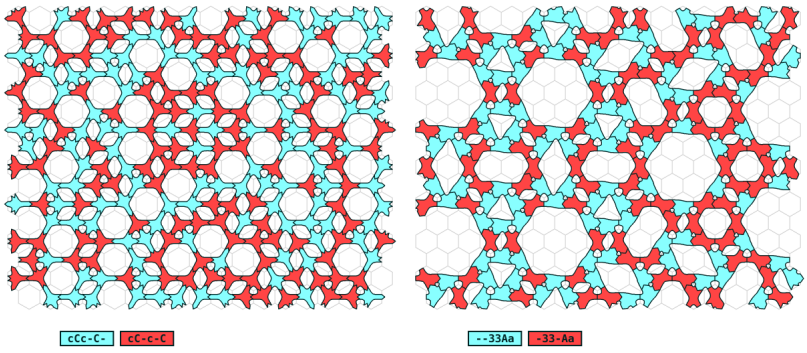

Figure 7.6: Tile sets the assembler has difficulty with.

The addition of one or two tiles to `AaAa--` (Figure 7.4) yields patterns

which when finite in size form Sierpinski Triangles (Figure 7.7).

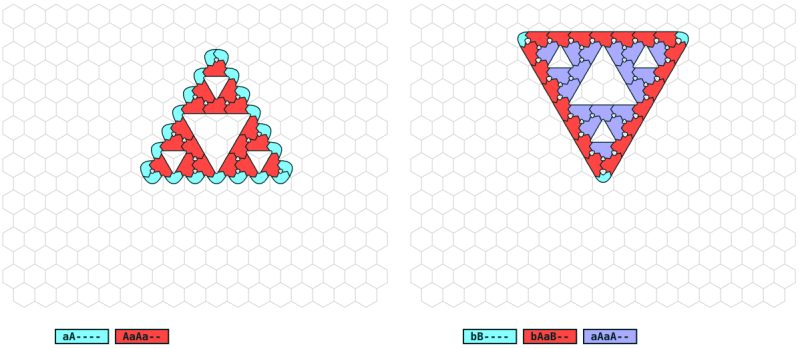

Figure 7.7: Tile sets that yield Sierpinski triangles.

The tile set in Figure 7.8 mimics the structure of DNA.[4] The tiles represent respectively the sugar-phosphate backbone, adenine, thymine, cytosine, and guanine.

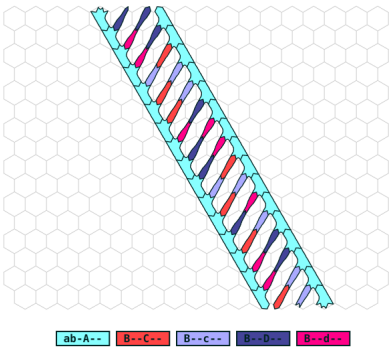

Figure 7.8: Tile set based on DNA.

The tile set on the left in Figure 7.9 is visually reminiscent of a Feynman diagram containing photons, electrons, and positrons. `c--C--` represents electrons and positrons, and `44----` represents photons. Relaxing the requirement that the assemblage be connected, and adding a tile for spontaneous electron-positron creation/annihilation gives rise to "zero-point fluctuations" (tile set on right).

[4]This tile set was suggested by Jeff Epler.

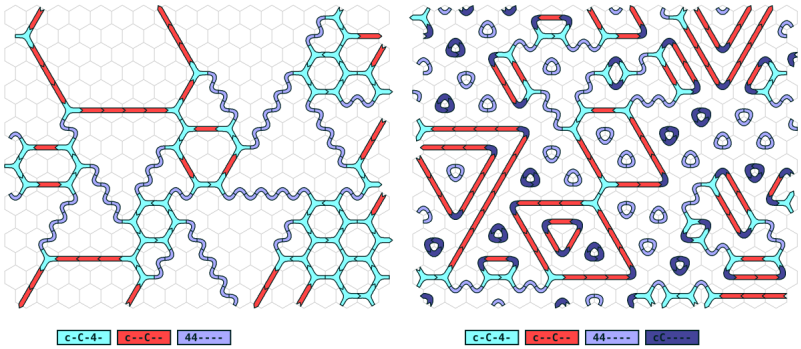

Figure 7.9: Tile sets reminiscent of Feynman diagrams.

Tile sets based on an underlying triangular grid may be simulated using a hexagonal grid (Figure 7.10). This merely requires that every second edge be empty.

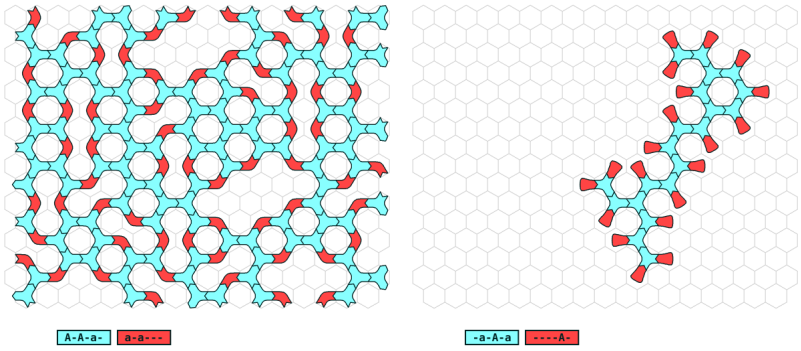

Figure 7.10: Tile sets based on triangles, simulated with hexagons.

If tiles are decorated by drawing lines connecting different edges, the results resemble Celtic knot-work (Figure 7.11).

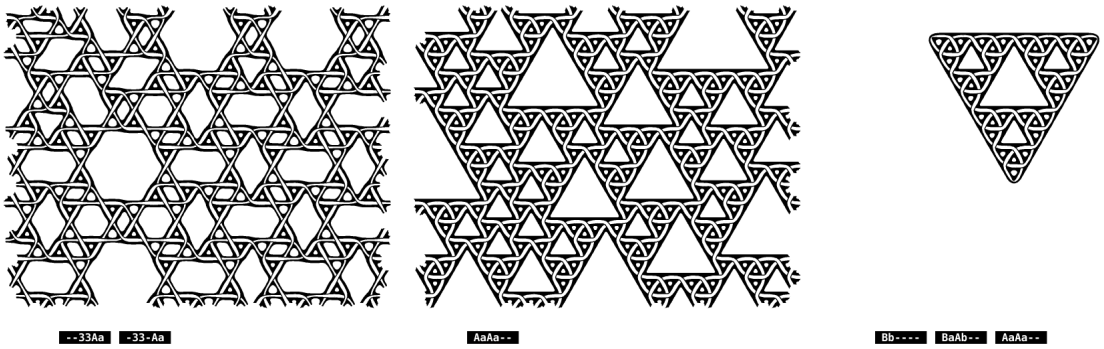

Figure 7.11: Knot-work patterns. The third pattern consists of a single loop.

7.4.3 k-morphism and crystallization

Grünbaum and Shephard [1987, pp.46–53] describe a number of tiles that allow multiple regular tilings. These are called k-morphisms. An example of this is shown in Figure 7.12. Tile sets were also found that suggest generalizations of this concept. Figure 7.13 shows a tile set that yields either regular tiling or a random network pattern. Figure 7.14 shows a tile set with ∞-morphism.

The assembly process (using the algorithm described earlier) shows behavior reminiscent of crystallization. The assembler initially makes little progress, but eventually produces a sufficient "seed" from which a pattern crystallizes outwards rapidly. This might also be considered a simple form of auto-catalysis.

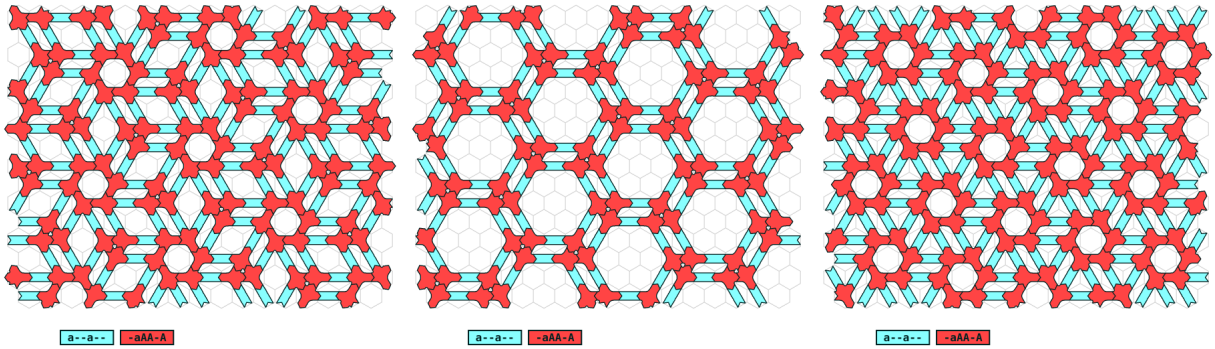

Figure 7.12: A k-morphic tile set. k is at least 3.

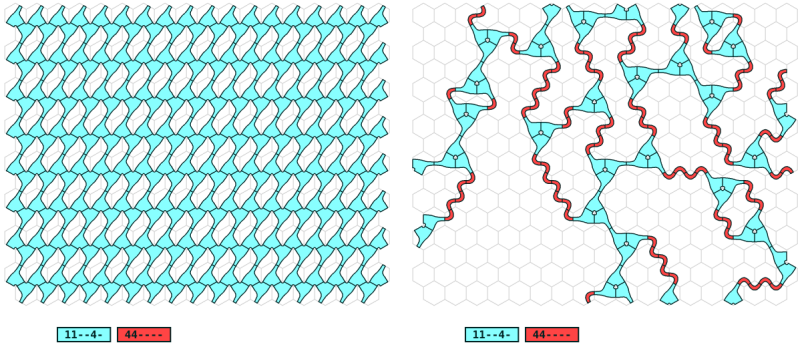

Figure 7.13: A tile set with two mutually exclusive modes.

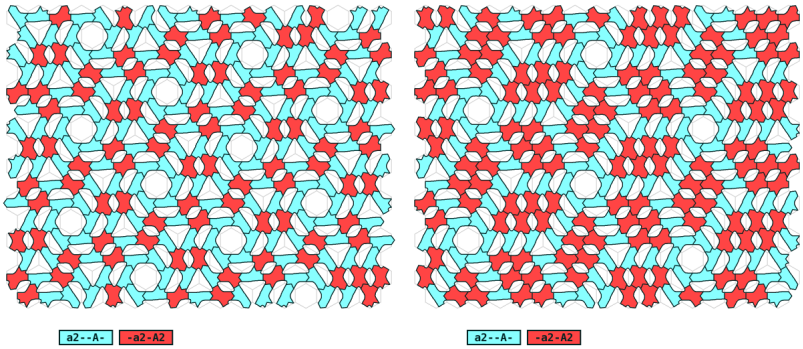

Figure 7.14: An ∞-morphic tile set. The repeating unit can be of arbitrary size.

7.5 Relation to cellular automata

A cellular automaton is a grid of cells in which each cell evolves over time according to simple local rules. By mapping the time dimension into a spatial dimension, appropriately shaped tile pieces can be used to implement cellular automata. This has interesting implications.

7.5.1 Wolfram's Elementary Cellular Automata

Wolfram's "Elementary Cellular Automata" [Wolfram, 2002] are one-dimensional automata in which each cell can be in one of two states, and in which the state of each cell depends only on the previous state of that cell and its two immediate neighbours. Such one-dimensional automata can be mapped into two-dimensional tile sets.

An Elementary Cellular Automaton tile set requires certain crossover pieces so that tiles implementing the rules of the automaton have access to all required input edges. The following tiles suffice: `a-aC-C`, `a-bC-D`, `b-aD-C`, `b-bD-D`.

A rule tile is required for each possible set of inputs, having three input edges as follows:

Input	Edges
000	cac
001	cad
010	cbc
011	cbd
100	dac
101	dad
110	dbc
111	dbd

Each rule tile will also have three output edges that represent the state of the cell, which must be one of:

State	Edges
0	AAA
1	BBB

The rule number of an Elementary Cellular Automaton when written in binary gives the mapping from inputs to states. For example, Rule 110 (Figure 7.15) maps to the tile set: `a-aC-C/a-bC-D/b-aD-C/b-bD-D/cacAAA/dacBBB/cbcBBB/dbcBBB/cadAAA/dadBBB/cbdBBB/dbdAAA`. Rule 110 has been shown by Matthew Cook to be capable of universal computation (see Wolfram [2002, pp. 675–689]).

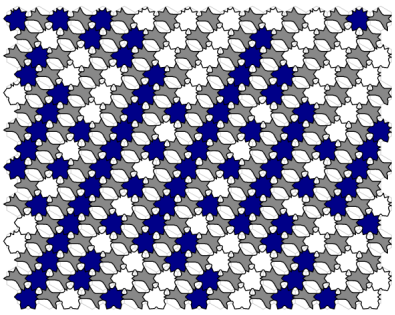

Figure 7.15: Elementary Cellular Automaton Rule 110, as a tile set.

7.5.2 Causality

In the case of tile sets based on cellular automata, a solution may be found without backtracking by selecting pieces in an order corresponding to the automata's time direction. Such tile sets might be described as causal. Furthermore these tile sets are deterministic, in that the anti-causal neighbours of a location fully determine which tile must be placed in it.

That causality is an emergent property of tile sets rather than an

assumption (as per cellular automata, and simulation of dynamic systems in general) allows us to think about cases that are "almost" deterministic-causal. There are two obvious ways to break strict deterministic causality:

- We might add several tiles that will match a given previous configuration. The result would be a random cellular automaton.
- We might choose not to include any tile which matches a certain input configuration. This would forbid any past state that would lead inevitably to this configuration. The result would be a tile set that is mostly causal, but with teleological elements.

Combining these two changes would yield a tile set that was "almost" deterministic causal. This would seem to be an interesting generalization. It would be interesting to know if teleological effects would tend to be obscured by random elements on sufficiently large scale in such a tile set.

The importance of this is not clear, and it is possible that it has no importance. The most obvious potential application would be in modelling quantum-scale phenomena. Entanglement, for example, is straightforward to implement in a near-causal tile-set. The discrete nature of tile-sets is also appealing at this scale. However it is not immediately clear how to account for destructive interference of the wave-function.

7.6 Discussion

A diverse range of patterns were formed from simple tile sets. This is evidence against Wolfram's claim that causality is necessary in order for

interesting patterns to be common. Though some tile sets are computationally difficult to assemble, many displaying interesting patterns are not, and these are not strictly those that can be generated in a causal manner. Causal systems are a class of easy-to-assemble tile sets, but there are likely to be other classes that yield patterns of comparable interest with comparable ease of assembly. For example, tile sets whose assembly by the algorithm described above sometimes requires a large backtrack, but on average require total backtracking of the order of the size of the assemblage, can be assembled in linear expected time.

Were the method of texture synthesis described in this chapter applied to decorating a (real or virtual) object, the nature of the tile-set would constrain the resulting decoration. One might even need to slightly redesign the object to suit the tile-set. A certain amount of back-and-forth would be required. It is the author's opinion that objects created using methods that require such back and forth can have greater aesthetic value than objects created using methods that do not. The patterns most difficult to work with may also be the ones of greatest aesthetic value.

There are interesting parallels between tile set patterns, Wolfram's cellular automata, and best-fit synthesis, all of which are instances of Markov Random Field synthesis. We saw in Chapter 3 that a goodness-of-fit metric based on the thin-tailed Gaussian distribution produced some characteristic results. Certain features would be repeated obsessively, in an almost autistic manner, and there were sometimes regions of "garbage" (this can be seen in Figure 2.6). These features disappeared when a more robust metric derived from the fat-tailed Cauchy distribution was used (Figure 3.4). A rule that says two pieces can not be placed next to each other unless they exactly match is also a kind of "thin tailed" criterion: the tail is so thin that it is zero! The rules of a Wolfram-style cellular automaton are another instance of this

– a particular rule either matches or it does not. Do we see these same characteristic patterns in cellular automata and tile set patterns? Yes. Excessive repetition is what Wolfram would call a glider. Indeed, in Figure 2.6, E3 displays features that are very clearly gliders (interpreting movement down the page as progression in time). And "garbage" is what Wolfram would call autoplectic randomness.

A criticism of Wolfram's work can be made on this basis. It is Wolfram's thesis that these kinds of features are seen in all forms of computation, and irrespective of the complexity of the underlying rules. However, Wolfram only studies discrete rules in detail, and these may all be characterized as "very thin tailed". More forgiving rules, such as the Cauchy-based metric introduced in Chapter 3 do not show these characteristics. "Thin-tailed" rules will tend to obsessively rely on only a small portion of the rule-set[5], so the size of the total rule set may not have much effect on the result. "Fat-tailed" rules, in which a rule is still applicable even if some criteria do not match exactly, will give rise to a more representative sampling of the total rule set, and may be capable of a richer set of behaviors.

For example, compare the best fit synthesis results for test image E3 using a Gaussian and Cauchy metric (Figure 7.16). With the heavier tailed Cauchy metric, the repeating "glider" patterns are reduced.

[5]In best-fit synthesis, the rule-set is derived from the contents of the texture image. Its complexity is proportional to the size of this image.

(a) 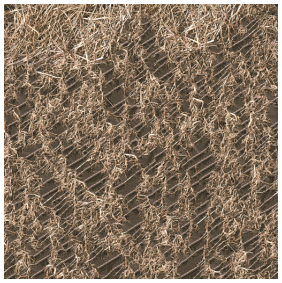 (b) 

Figure 7.16: Test image E3 synthesized using Garber's method. (a) original metric, (b) Cauchy metric ($\sigma = 15$).

Interestingly, a causal relation between elements does not seem necessary in order to produce this "autistic" behavior. The tile set patterns of this chapter also contain repeating "gliders", and multiple modes (k-morphism) which lock themselves in such that a pattern can not be extended to form a transition to a different mode. The best-fit variant described in Chapter 3 also approximates acausality by choosing pixels in random order and by refining early chosen pixel values on the basis of later chosen ones, yet still produces obsessive repetitions when the Gaussian derived metric is used.

Chapter 8

Conclusion and future work

In the introduction, three texture operations were identified: texture synthesis, texture transfer, and plausible restoration. This dissertation has presented several different approaches to performing these operations:

- A variant of the best-fit method that is fast and flexible, capable of all three operations (Chapter 3).
- A fast patchwork synthesis method, capable of texture synthesis and transfer (Chapter 5).
- A method based on texture modelling, capable of plausible restoration of both missing areas and noise corrupted images (Chapter 6).

These represent different trade-offs between speed, quality, and generality. In particular, the best-fit variant described in Chapter 3 represents a practical approach to these operations in a wide range of circumstances, and is in current use as a GIMP plug-in.

Some theoretical aspects of texture synthesis were also explored using tile patterns (Chapter 7). This served to place methods of performing the texture operations presented here and elsewhere in context.

An image, even if damaged, contains a great deal of information about its texture. As the methods of Chapters 3 and 6 demonstrated, this information may be extracted from the image and used to repair or alter it. We need not pre-program into methods of performing texture operations specific information about the types of features found in images (such as that they might contain sharp edges, or spot and edge features of different scales), as this information is already present in the image. Indeed to specify these things a priori may limit the range of images a method can successfully operate on.

Methods such as the plausible restoration method of Chapter 6 may eventually out-perform the best-fit method and variants, as such methods are capable not just of copying existing areas of texture but inventing new plausible instances of that texture based on an inferred model of the texture. For example, such methods may extrapolate pixel values outside of the bounds seen in the available texture sample (see Figure 6.5). A major weakness with the method presented in Chapter 6, however, is that it is one of finding a unique optimum. The best-fit methods, by contrast, sample from a field of possibilities. The method of Chapter 6 can therefore reconstruct smooth curves, but not replicate the roughness of the original texture.

To remove this weakness, the merit function (Equation 6.4) would need to be replaced by an explicit probability density function, and random samples produced based on that function. A random sample might be produced from such a probability density function using the Metropolis-Hastings algorithm (see Section 2.2.2). Such an extension would also allow the method of Chapter 6 to be applied to texture

synthesis and texture transfer. However, given the large number of parameters involved (one parameter per pixel of the image, plus the parameters of the model), a naive application of this algorithm will take an unreasonable number of iterations to converge. Finding a variant of the Metropolis-Hastings algorithm that converges quickly is an open problem.

An interesting feature of the texture operations identified in the introduction is that they can bypass modelling. To predict the value of some unknown data we normally select a model based on the data we have available (induction) and use this model to predict the unknown data (deduction). There is a problem, however, with deciding exactly which model to use. If the most likely model is chosen (Maximum Likelihood), we have ignored the possibility that the data was a less likely product of a slightly less likely model. The Maximum Likelihood model will tend to *over-fit* the data. Statisticians avoid over-fitting by using "unbiased" estimators of model parameters. An unbiased estimator is a means of estimating a parameter such that the average expected value of the estimator, when applied to a sample of any size, is equal to the true value of the parameter [McGee, 1971, pp.99–100]. An unbiased estimate may be found for any single parameter in a model, but combining these estimates into a full model does not produce an unbiased model. For example, if a texture sample were insufficiently large to allow a decision between two different possible models of texture, a model composed of unbiased parameters might—incorrectly—allow a mixture of the two possible textures in a single image. This problem will occur in any method that tries to use a single model to characterize the field of all possible models.

However, when performing the texture operations, we need not settle on a specific model. The output of the texture operations is a random sample from the field of all possible results. Methods of performing

texture operations may choose a model at random (conformant to the probability distribution of models given the input data), or omit modelling entirely. The best-fit method omits modelling, producing new samples directly from the sample given.[1] If the method of Chapter 6 were extended to perform sampling, as described above, the sample produced would have an associated randomly sampled model.

Beyond sampling from the field of possible images, we may wish to characterize the full field. This would be useful where we need to be sure that what we are reconstructing is really there, and not just a plausible confabulation (for example, in medical or military applications). We may wish to find the average image, or measure the amount of possible variation in a particular region, or calculate some other relevant statistics. For example, in Figure 6.3, some fine texturing in the hat was lost. The values of pixels in the hat in the image of maximum likelihood happen to lie at the boundary of their allowed ranges, and are not representative of the field of possibilities. An average of the field would be more representative, and would preserve this fine texturing without inventing new details.

In conclusion, significant progress has been made in this dissertation towards the ideal of an all-purpose texture tool, and has also mapped out some fundamental challenges that must be taken into account when creating such tools. Ongoing development of more powerful tools will provide a richer environment of interactions between artists and designers and the objects they create, helping better express both the intentions of artists and designers and the underlying logic of the textures with which they work.

[1] To produce a truly random sample, the best-fit method would need to examine previously synthesized areas of the output in addition to the input. The plausible restoration method described by Drori et al. [2003] does this.

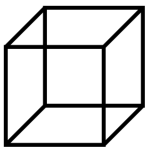

Appendix A

Test suites

In this dissertation, various texture operations needed to be tested. For this purpose, a test-suite of images was selected. Also, images suitable for texture transfer were selected.

A.1 Images

A test suite of images was chosen from the VisTex texture database [VisTex]. These are shown in Figure A.1. Included are simple (S1, S2) and complex (C1, C2, C3, C4) textures, textures with elongated features (E1, E2, E3), tiling patterns (T1, T2), and several images with non-homogeneous texture (N1, N2, N3). All images contain 256×256 pixels.

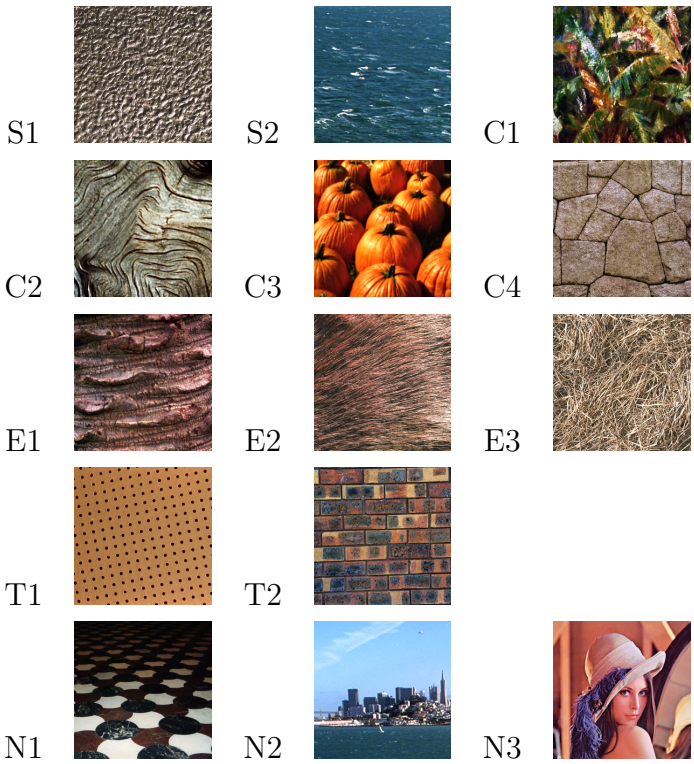

Figure A.1: Test suite for texture synthesis.

A.2 Texture transfer

Test images for texture transfer were also selected. The two textures (Figure A.2a) were taken from the VisTex database [VisTex] and are both 512×512 pixels in size. The pattern images (Figure A.2b) were taken with a digital camera, and are 825×630 and 548×804 pixels in size respectively.

(a) S1  S2 

(b) I1  I2 

Figure A.2: Texture transfer test suite: (a) texture samples, (b) images.

Appendix B

Paper presented at WSCG-2001

The following paper was presented at WSCG-2001, a computer graphics conference held at the University of West Bohemia in the Czech Republic. It describes an early and overly complicated attempt at tackling the problems addressed in Chapter 3.

Google Scholar[1] lists 22 citations of this paper by other authors.

[1] `http://scholar.google.com/`

A NON-HIERARCHICAL PROCEDURE FOR RE-SYNTHESIS OF COMPLEX TEXTURES

Paul Harrison

School of Computer Science and Software Engineering
Monash University
Wellington Rd.
Clayton, 3800
Melbourne, Australia
pfh@yoyo.cc.monash.edu.au

ABSTRACT

A procedure is described for synthesizing an image with the same texture as a given input image. To achieve this, the output image is built up by successively adding pixels selected from the input image. Pixels are chosen by searching the input image for patches that closely match pixels already present in the output image. It is shown that the accurate reproduction of features in the input texture depends on the order in which pixels are added to the output image. A procedure for selecting an ordering which transfers large complex features of the input to the output image is described. This procedure is capable of reproducing large features even if only the interactions of nearby pixels are considered. The procedure can be altered to allow specification of the placement of particular features in the output texture. Several applications of this are described.

Keywords: texture synthesis, image manipulation

1 INTRODUCTION

The texture of an image might be defined broadly as the interrelationships between pixels in that image. The ability to analyse and manipulate image texture has a number of interesting applications. The simplest application is to create a new image with the same texture but of different size and shape to a sample image. Seamless editing of images is also a possibility. For example an object could be removed from an image by synthesizing a new section of the background texture over the top of it. These applications all rely on the ability to re-synthesize a sample texture to fit a variety of constraints.

A number of texture re-synthesis methods are described in the literature. One approach is based on searching for specific features in textures [Heege95] [Bonet97] [Porti99]. In these methods, the input image is decomposed into a set of features. Statistics about these features are collected, and used to synthesize a new image. One problem with these methods is that they can only recognize a set of features which have been specified in advance. While the results can be impressive, it is difficult to devise a generic feature set that can be used to describe all textures.

Another approach to the texture re-synthesis problem is to analyse and reproduce interactions between individual pixels [Monne81] [Gagal90]. Methods based on this approach define a function describing a pixel in terms of its neighbours and a random element. This function is used to generate a new image, pixel by pixel.

Recently, a new pixel-based technique has been developed based on best-fit searching. Garber [Garbe81] and Efros and Leung [Efros99] independently developed this approach, in which each pixel is selected by searching the input image for a patch of pixels closely matching nearby pixels already present in the output image. This results in an output image pieced together from small parts of the input image. Using this technique, textures can be synthesized in which the relationships between neighbouring pixels are extremely

Ω_I :	The set of pixel locations in the input image.
$I(s)$, $s \in \Omega_I$:	The pixel in the input image at location s.
Ω_O :	The set of locations containing pixels in the output image.
$O(s)$, $s \in \Omega_O$:	The pixel in the output image at location s.
$L(s)$, $s \in \Omega_O$:	The location of the pixel in the input image that is in the output image at location s.
Ω_K :	The set of offsets considered when calculating the similarity of two texture patches.
$K(u)$, $u \in \Omega_K$:	Weighting given to a particular offset u.
$A(s)$, $s \in \Omega_I$	
$B(s)$, $s \in \Omega_O$:	Two uniformly random functions.

Table 1: Table of symbols.

complex.

Efros and Leung report that for good results the size of the patch searched for in the input image should correspond to the size of the largest feature in the texture. To allow larger features, Wei and Levoy [Wei00] propose a hybrid of the feature-based and best-fit techniques that generates the output in a pyramid of successively finer resolutions.

This paper presents a refinement of the pixel-based best-fit re-synthesis procedures introduced by Garber [Garbe81] and Efros and Leung [Efros99]. The most important change is to the selection of the order in which pixels are added to the output image. This order is selected to allow reproduction of features larger than the size of the patches searched for in the input image. The procedure avoids decomposing the input image into a predefined feature set, and can therefore re-synthesize a wide range of textures. An extension to this procedure is presented that allows specification of the layout of different regions of texture in the output image.

2 RE-SYNTHESIS PROCEDURE

The procedure described in this paper takes as input an image containing a sample of a texture and produces another image with the same texture.

The procedure has two stages. In the first stage, pixel interrelationships in the input image are analysed. The extent to which the value of each pixel constrains the values that can be taken by neighbouring pixels is determined. The reasons for doing this are discussed in section 2.1 and the calculations necessary are described in section 2.2.

In the second stage, pixels are added to the initially blank output image until all locations have been filled. The order in which pixels are added is chosen to facilitate faithful reproduction of the texture of the input image, using the results from the first stage, as described in sections 2.1 and 2.2.1. Section 2.2.1 also describes the initialization of this stage in terms of choice of the locations and values of seed pixels.

To add a pixel to the output image at a particular location, the surrounding pixels which have already been added to the output image are examined. The closest match to these pixels is located in the input image, and the corresponding pixel from the input image is inserted in the output. This is described below and in section 2.2.2.

Symbols used in this paper are listed in Table 1.

Colours are stored as RGB values. To compare individual pixels, the sum of the absolute values of the differences in each colour component was used:

$$d((r_1, g_1, b_1), (r_2, g_2, b_2)) = |r_2 - r_1| + |g_2 - g_1| + |b_2 - b_1| \quad (1)$$

To measure how closely patches from the input image match a patch in the output image, a distance function can be used. The distance function used in this paper is a weighted Manhattan (city block) distance function. To allow synthesis of textures with a random element, the distance function contains a small random component with weight specified by the parameter ε:

$$D(s,t) = \varepsilon\,|A(s) - B(t)| + \sum_{u \in \Omega_K, t+u \in \Omega_O} K(u)\, d(I(s+u), O(t+u)) \quad (2)$$

The Manhattan distance was chosen over the more commonly used Euclidean distance as it is more forgiving of outliers. I.e. a good match in most pixels in the patch will not be negated by a poor match in one or two pixels.

Figure 1: Barcode texture.

For each location t in the output image, a pixel $I(s)$ from the input image is chosen. The location s in the input image is selected to minimize the distance $D(s,t)$ as given in Eq. 2.

2.1 Ordering of pixel insertion

This section discusses the order in which pixels are added to the output image in the second stage of the procedure. As will be demonstrated, certain features such as branching patterns are only reproduced correctly in the output image if the placement of pixels proceeds in a particular order.

Consider the values a particular pixel in a textural image could take. The pixel value must be consistent with the values of all other pixels in the image. These other pixels may be said to constrain the values the selected pixel can take.

An important property of these constraints is that the constraint imposed by a distant pixel in some direction may also be provided by a closer pixel in the same direction. In general, most of the constraint will be imposed by nearby pixels. For example, in Fig. 1 the constraint imposed by pixels far above or below a given pixel will also be provided by pixels a small distance above or below that pixel. This kind of relationship may be directional. In Fig. 1 it applies vertically but not horizontally.

These constraints can be thought of in terms of information theory [Blahu87]. Without any prior knowledge, a pixel is equally likely to take any value, and this requires a certain number of bits to encode. If its neighbours impose constraints on the values it can take, it will require (on average) less bits to encode. The average number of bits required to encode some information is referred to as its *entropy* [Blahu87, pp. 55]. Entropy can therefore be used to measure the constraints imposed on a pixel.

The pixel selection procedure is based on a search for patches of pixels in the input image that match those already placed in the output. These patches must cover enough pixels to capture all

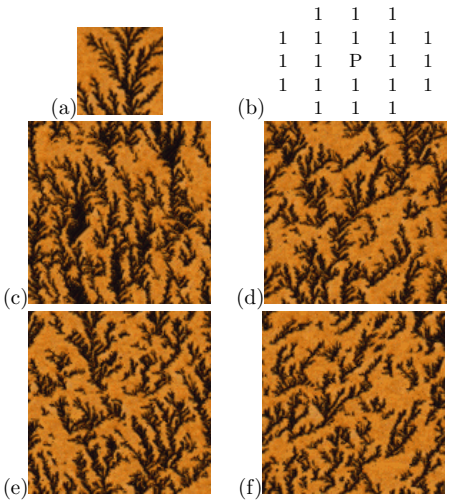

Figure 2: Textures generated using different orders of pixel insertion.
Input image (a), weighting of the distance function $K(u)$ used about the center pixel P (b), and the output from raster scans proceeding from top to bottom (c), bottom to top (d), left to right (e), and right to left (f).

the constraints on each location, or the texture will not be reproduced correctly. However, if the patch size is too large, there will be less chance of finding good matches in the input image. It is therefore desirable to choose an order to add pixels to the output image in which the constraints imposed on each location are captured by a small neighbourhood of pixels.

One order that can be used to add pixels is a raster scan. Fig. 2 shows images generated using raster scans in different directions. The lichen texture being synthesized has a complex branching pattern. As can be seen, the scan that proceeds from bottom to top (Fig. 2d) reproduces this pattern the most accurately.

The other raster scans in Fig. 2 have various problems. The top to bottom scan (Fig. 2c) produces anomalous dark blotches, and the lichen in the sideways scans (Fig. 2e and 2f) have branches on one side only.

These artifacts can be explained by considering how the pixels constrain one another. The constraint imposed on a given pixel by the pixels immediately below it is almost the same as the constraint imposed by all pixels below it. This is not true of pixels above or to either side of that pixel. The bottom-to-top raster scan therefore produces

a better result than the others tested.

To utilize these types of constraint, the resynthesis procedure assigns a priority to each location in the output image. Highest priority is given to locations which are highly constrained by neighbouring pixels that have already been added. Then the following procedure is followed:

```
While there are still empty locations in
 the output image:
    • Find the empty location with the
      highest priority.
    • Choose a pixel from the input image
      to place in that location.
    • Update priorities of empty
      neighbouring locations based on the
      new pixel value.
```

A system for assigning priorities needs to be chosen. A simple prioritization scheme estimates the entropy of each unfilled location given its nearby neighbours, and gives higher priority to locations with lower entropy. The problem with this scheme is that there may be some areas of a texture in which nearby pixels tightly constrain each other, and others where there is less constraint and pixel values are more random. The areas with tight constraints will always be given higher priorities and therefore be disproportionately represented in the output image.

The approach taken in this paper is to define a normalized weighting $W(s,u)$. This weighting indicates the relative amount of information a pixel $I(s)$ gives about each of its neighbours $I(s+u)$. To ensure no part of the image is given an advantage over another part, this weighting is defined so that it sums to unity for each pixel $I(s)$. The priority of each empty location in the output can then be defined as a sum of the weightings from neighbouring pixels.

2.2 Analysing interactions between neighbouring pixels

Weightings are needed to prioritize the order in which pixels are inserted. They are also needed in the distance function used to select these pixels. To create these weightings, interactions between neighbouring pixels in the input image are analysed. The calculation of these weightings is the first stage of the synthesis procedure. For purposes of computational simplicity, the effect of each neighbour on a location is assumed to be independent of the effects of other neighbours. The interactions between constraints of different neighbours on a location are neglected.

To compute the weightings, the amount of information every pixel provides about each of its near neighbours first needs to be estimated. The neighbours being considered are those whose offset from the central pixel is a member of the set of offsets Ω_K used to calculate the distance function $D(s,t)$ (Eq. 2).

These amounts of information may be measured by considering each offset $u \in \Omega_K$ in turn. For each offset, the number of bits of information $G(s,u)$ provided by each pixel in the input image $I(s)$ about the pixel offset from it $I(s+u)$ is estimated, as explained below.

Offset pixels $I(s+u)$ are grouped into sets based on the value of the corresponding pixel $I(s)$. Within each set, the pixels will have a distribution of values. These values are modelled as being normally distributed in each colour component (red, green and blue), and the parameters of these distributions are estimated. This is used to calculate the number of bits required to encode pixels of each set.

To distribute the pixels $I(s+u)$ into sets, they are classified by the most significant m bits of the red, green and blue components of $I(s)$. The value of m should be chosen so that the sets are neither so small that an accurate estimate of the mean and standard deviation is impossible, nor so large that most of the information from $I(s)$ is discarded.

If it is assumed that all the pixels in a set come from the same distribution, standard deviations calculated from the sets can be used to describe individual pixels in those sets. This gives standard deviations for each pixel at each offset for each colour component: $\sigma_r(s,u)$, $\sigma_g(s,u)$, $\sigma_b(s,u)$.

These standard deviations can be used to calculate the entropy of each pixel $I(s+u)$ given $I(s)$. The average number of bits required to store a normally distributed variable with standard deviation σ, to an accuracy of $\pm\frac{1}{2}$, is:

$$\frac{1}{2}\log_2(2\pi) + \frac{1}{2\ln 2} + \log_2\sigma \qquad (3)$$

Summing this for each colour component gives the entropy of the pixel $I(s+u)$ given $I(s)$:

$$H(s,u) = \begin{array}{l} \frac{3}{2}\log_2(2\pi) + \frac{3}{2\ln 2} \\ +\log_2\sigma_r(s,u)\sigma_g(s,u)\sigma_b(s,u) \end{array} \qquad (4)$$

Performing the same calculation without splitting the image into sets gives the entropy of pixels in the image independent of any of their neighbours, H_{image}.

The number of bits given by a pixel $I(s)$ about another pixel offset from it $I(s+u)$ can then be found by subtracting the entropy of $I(s+u)$ given $I(s)$ from the entropy of pixels in the image if nothing is known about their neighbours. Call this value $G(s,u)$, where:

$$G(s,u) = H_{image} - H(s,u) \tag{5}$$

2.2.1 Prioritization weighting

A normalized weighting $W(s,u)$ suitable for prioritizing the order in which pixels are added to the output image can be defined from $G(s,u)$:

$$W(s,u) = \frac{G(s,u)}{\sum_{-v \in \Omega_K} G(s,v)} \tag{6}$$

The priorities of unfilled locations in the output image may be defined from $W(s,u)$:

$$P(s) = \sum_{u \in \Omega_K, s+u \in \Omega_O} W(L(s+u), -u) \tag{7}$$

Additionally, locations near the edge of the image have their priorities adjusted as if the positions beyond the edge of the image were already filled by pixels having average properties (i.e. with weights $W(s,u)$ averaged over all s). These locations then act as starting positions for filling the output image. The value of the first pixel added, having no neighbours, is chosen at random from the input image (on the basis of the random component of the distance function).

2.2.2 Distance function weighting

The distance function $D(s,t)$ (Eq. 2) used to select pixels also requires a set of weightings. To make best use of the input image, these weightings should reflect the degree to which each neighbour constrains the value of the pixel.

The entropy of a normally distributed random variable, such as one of the color components of a pixel, is the logarithm to base two of its standard deviation, to within a constant (see Eq. 3). This means that for each time a constraint on a particular location halves the standard deviation of possible values of one color component of that location, one more bit of information about the location becomes known. In light of this relationship, the weighting given to a neighbour might be doubled for every bit it gives about a location.

The weighting system used in the distance function was chosen to satisfy this constraint:

$$K(u) = 2^{G(-u)} \tag{8}$$

where $G(u)$ is the average value of the weightings $G(s,u)$ for a particular offset u.

2.3 Results of the procedure

Example results from the procedure are shown in Fig. 3. A seven by seven neighbourhood of pixels ($\Omega_K = [-3,3] \times [-3,3]$) was used to generate these images.

The images in Fig. 3 required an average of four and a half minutes and six and a half megabytes of memory to produce on a 300Mhz Pentium II. The time taken by the procedure increases approximately linearly with the size of the input image, and can be extremely slow for large input images.

Less successful results are shown in Fig. 4. In particular the procedure is very sensitive to features that only appear at the edge of the input image. In this case the output tends to contain artifacts such as repeating patterns. Also, as can be seen in Fig. 4b, the procedure does not recognize regularly spaced components of a texture such as tiles.

3 SPECIFICATION OF THE PLACEMENT OF TEXTURE REGIONS

Some textures contain several regions, with properties that differ from one region to another. A simple extension to the distance function used to select pixels gives a means of specifying the layout of these regions in the output image. This extension requires the definition of two new images, one which maps regions in the input, $J(s)$, and one which specifies corresponding regions in the output, $Q(t)$. It also requires weightings, $L(u)$,

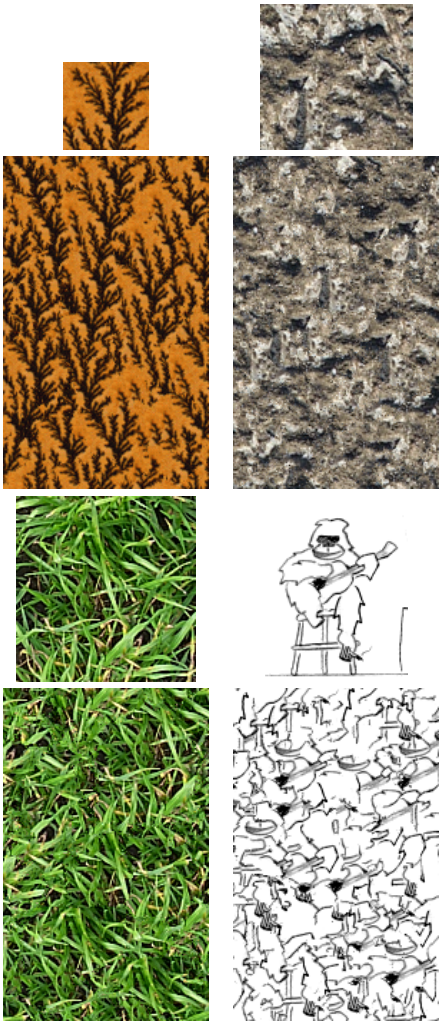

Figure 3: Sample results.
The output of the procedure is shown below each input image.

which represent the relative importance of pixels from the input map in determining the value of their surrounding pixels in the input image. These are chosen using the same method as that used to choose $K(u)$. Then a new distance function is used in place of Eq. 2:

$$D(s,t) = \varepsilon\,|A(s) - B(t)| + \sum_{u\in\Omega_K, t+u\in\Omega_O} \{K(u)d(I(s+u), O(t+u)) + L(u)d(J(s+u), Q(t+u))\} \quad (9)$$

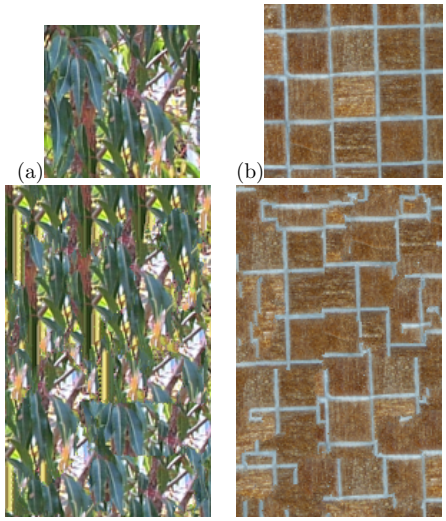

An implementation of the procedure can be obtained from `http://www.csse.monash.edu.au/~pfh/resynthesizer/`

Figure 4: Some failures.

3.1 Results of the extended procedure

An example of the use of the extended synthesis procedure is shown in Fig. 5. The texture used was a photograph of clouds (Fig. 5b). A map of this texture was created showing regions of cloud and blue sky (Fig. 5a). Another map, of a checkerboard pattern, was used as the output map (Fig. 5c). The result of applying the procedure to these three images is shown in Fig. 5d.

Texture re-synthesis has been previously applied to the removal of objects on a homogeneous background by synthesizing a new section of that background [Igehy97] [Efros99]. The ability to constrain placement of texture regions allows synthesis of a new background to replace an object, even if the background is non-homogeneous. An example of this is shown in Fig. 6. Fig. 6a shows a picture of a donkey standing in a field. In this picture, the field is not homogeneous because of perspective expansion. A feature map of the image (Fig. 6b) was constructed with parts of the image equidistant from the camera having the same value. A new section of the background was then synthesized to replace the donkey, using the rest of the background as input texture. The new section was constrained to join with the existing background and to follow the feature map. The

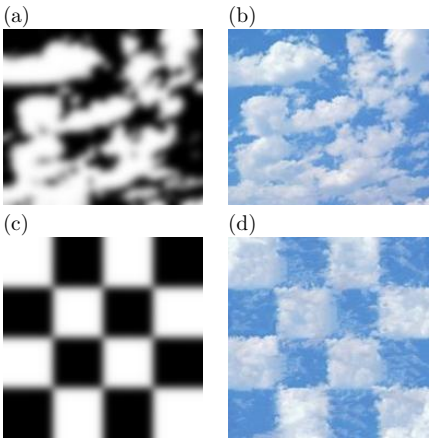

Figure 5: Constraining a cloud texture to a checkerboard pattern.
Input map (a), input texture (b), output map (c), and output of the extended synthesis procedure (d).

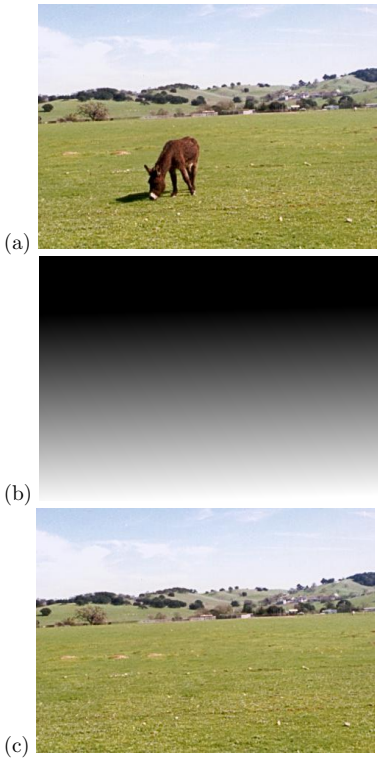

Figure 6: Example of object removal.
Original image (from [Igehy97]) (a), map (b), and image with object removed (c).

result is shown in Fig. 6c.

4 CONCLUSION AND FUTURE WORK

A procedure has been described for synthesizing an image of arbitrary size with the same texture as that of a sample input image. The procedure is capable of reproducing large features from this input image, even though it only examines interactions between pixels that are close neighbours. Significantly, the procedure does not have any preconceived notion of what features to expect in the input texture.

A simple extension to this procedure allows feature placement in the new image to be constrained. It is effectively a generic filter, in that when given an example of a change to one image it can reproduce the same change in another image.

Future work on the procedure described here could refine the distance function to consider matches that have similar structure even if they are slightly lighter or darker or have a different hue. It could also be extended to work on non-flat geometries, to allow synthesis of textures covering three-dimensional objects. It might also be applied to three dimensions to manipulate animations or solid textures, or to one dimension as a sound synthesis technique.

ACKNOWLEDGEMENTS

I thank my P.h.D. supervisor, Dr. Alan Dorin, for his patience and for many helpful suggestions. I also thank Homan Igehy and Lucas Pereira for the use of one of their images in this paper.

REFERENCES

[Blahu87] R. E. Blahut. *Principles and Practice of Information Theory.* Addison-Wesley, 1987.

[Bonet97] J. S. De Bonet. Multiresolution sampling procedure for analysis and synthesis of texture images. In *Proceedings of SIGGRAPH 1997*, pages 361–368, 1997.

[Efros99] A. A. Efros and T. K. Leung. Texture synthesis by non-parametric sampling. In *Proceedings of the 7th IEEE International Conference on Computer Vision*, pages 1033–1038, 1999.

[Gagal90] A. Gagalowicz and S. De Ma. Sequential synthesis of natural textures. In *Selected Papers on Digital Image Processing*,

pages 184–210. SPIE Optical Engineering Press, 1990.

[Garbe81] D. Garber. *Computational Models for Texture Analysis and Texture Synthesis*. PhD thesis, University of Southern California, 1981.

[Heege95] D. J. Heeger and J. R. Bergen. Pyramid-based texture analysis/synthesis. In *Proceedings of SIGGRAPH 1995*, pages 229–238, 1995.

[Igehy97] H. Igehy and L. Pereira. Image replacement through texture synthesis. In *Proceedings of the 1997 IEEE International Conference on Image Processing*, 1997. Available: `http://graphics.stanford.edu/papers/texture_replace/` (Accessed: 2000, September 7).

[Monne81] J. Monne, F. Schmitt, and D. Massaloux. Bidimensional texture synthesis by Markov chains. *Computer Graphics and Image Processing*, 17:1–23, 1981.

[Porti99] J. Portilla and E. P. Simoncelli. Texture modeling and synthesis using joing statistics of complex wavelet coefficients. In *Proceedings of the IEEE Workshop on Statistical and Computational Theories of Vision*, 1999. Available: `http://www.cis.ohio-state.edu/~szhu/SCTV99.html` (Accessed: 2000, September 7).

[Wei00] L. Wei and M. Levoy. Fast texture synthesis using tree-structured vector quantization. In *Proceedings of SIGGRAPH 2000*, 2000. Available: `http://graphics.stanford.edu/projects/texture/` (Accessed: 2000, September 7).

Bibliography

M. Ashikhmin. Synthesizing natural textures. In *Proceedings of the ACM Symposium on Interactive 3D Graphics*, pages 217–226. ACM Press, 2001.

M. Ashikhmin. Fast texture transfer. *IEEE Computer Graphics and Applications*, 23(4):38–43, 2003.

J. R. Bergen and E. H. Adelson. Early vision and texture perception. *Nature*, 333:363–364, May 1988.

V. Bhaskaran and K. Konstantinides. *Image and Video Compression Standards*. Kluwer Academic Publishers, 1995.

C. Blakemore and G. F. Cooper. Development of the brain depends on the visual environment. *Nature*, 228:477–478, 1970.

S. Brin. Near neighbour search in large metric spaces. In *Proceedings of the 21st International Conference on Very Large Data Bases*, pages 574–584, Zurich, Switzerland, 1995. Morgan Kaufmann Publishers.

R. Chellappa and R. L. Kashyap. Texture synthesis using 2-d noncausal autoregressive models. *IEEE Transactions on Acoustics, Speech, and Signal Processing*, 33(1):194–203, February 1985.

M. F. Cohen, J. Shade, S. Hiller, and O. Deussen. Wang tiles for image and texture generation. In *Proceedings of SIGGRAPH 2003*, pages 287–294. ACM Press, 2003.

P. L. Combettes. Image restoration subject to a total variation constraint. *IEEE Transactions on Image Processing*, 13(9):1213–1222, 2004.

A. Criminisi, P. Perez, and K. Toyama. Region filling and object removal by examplar-based image inpainting. Technical Report MSR-TR-2003-84, Microsoft Corporation, 2003.

K. Culik. An aperiodic set of 13 wang tiles. *Discrete Mathematics*, 160: 245–251, 1996.

J. S. DeBonet. Multiresolution sampling procedure for analysis and synthesis of texture images. In *Proceedings of SIGGRAPH 1997*, pages 361–368. ACM Press, 1997.

I. Drori, D. Cohen-Or, and H. Yeshurun. Fragment-based image completion. In *Proceedings of SIGGRAPH 2003*, pages 303–312. ACM Press, 2003.

D. S. Ebert, F. K. Musgrave, D. Peachy, K. Perlin, and S. Worley. *Texturing and Modelling: a procedural approach*. Academic Press Inc., 1994.

A. A. Efros and W. T. Freeman. Image quilting for texture synthesis and transfer. In *Proceedings of SIGGRAPH 2001*, pages 341–346. ACM Press, 2001.

A. A. Efros and T. K. Leung. Texture synthesis by non-parametric sampling. In *Proceedings of the 7th IEEE International Conference on Computer Vision*, pages 1033–1038. IEEE, 1999.

C. Fearnley. *Where have all the Textures gone?* John McIndoe Ltd, 1975.

J. H. Friedman. An algorithm for finding best matches in logarithmic expected time. *ACM Transactions on Mathematical Software*, 3(3): 209–226, September 1977.

D. Garber. *Computational Models for Texture Analysis and Texture Synthesis*. PhD thesis, University of Southern California, 1981.

M. Ghazel, G. H. Freeman, and E. R. Vrscay. Fractal image denoising. *IEEE Transactions on Image Processing*, 12(12):1560–1578, 2003.

G. Gilboa, N. Sochen, and Y. Y. Zeevi. Forward-and-backward diffusion processes for adaptive image enhancement and denoising. *IEEE Transactions on Image Processing*, 11(7):689–703, 2002.

B. Grünbaum and G. C. Shephard. *Tilings and Patterns*. W. H. Freeman and Company, 1987.

P. F. Harrison. A non-hierarchical procedure for re-synthesis of complex textures. In *WSCG'2001*, pages 190–197, Plzen, Czech Republic, 2001. University of West Bohemia.

D. J. Heeger and J. R. Bergen. Pyramid-based texture analysis/synthesis. In *Proceedings of SIGGRAPH 1995*, pages 229–238. ACM Press, 1995.

C. W. Helstrom. Image restoration by the method of least squares. In *Selected Papers on Digital Image Processing*, pages 619–625. SPIE Optical Engineering Press, 1990.

A. Hertzmann, C. E. Jacobs, N. Oliver, B. Curless, and D. H. Salesin. Image analogies. In *Proceedings of SIGGRAPH 2001*. ACM Press, 2001. Available: `http://mrl.nyu.edu/projects/image-analogies/` (Accessed: 2002, May 31).

D. H. Hubel and T. N. Wiesel. Receptive fields, binocular interaction and functional architecture in the cat's visual cortex. *Journal of Physiology*, 160:106–154, 1962.

H. Igehy and L. Pereira. Image replacement through texture synthesis. In *Proceedings of the 1997 IEEE International Conference on Image*

Processing. IEEE, 1997. Available: `http://graphics.stanford.edu/papers/texture_replace/` (Accessed: 2000, September 7).

B. Julesz and B. Kröse. Features and spatial filters. *Nature*, 333: 302–303, 1988.

I. Keys. *The Texture of Music: from Purcell to Brahms*. Dobson Books Ltd, 1961.

V. Kwatra, A. Schödl, I. Essa, G. Turk, and A. Bobick. Graphcut textures: Image and video synthesis using graph cuts. In *Proceedings of SIGGRAPH 2003*, pages 277–286. ACM Press, 2003.

J. Lee. Digital image enhancement and noise filtering by use of local statistics. *IEEE Transactions on Pattern Analysis and Machine Intelligence*, PAMI-2(2):165–168, 1980.

L. Liang, C. Liu, Y. Xu, B. Guo, and H. Shum. Real-time texture synthesis by patch-based sampling. *ACM Transactions on Graphics*, 20:127–150, 2001.

R. Llados-Bernaus, M. A. Robertson, and R. L. Stevenson. A stochastic technique for the removal of artifacts in compressed images and video. In *Signal Recovery Techniques for Image and Video Compression and Transmission*, pages 35–68. Kluwer Academic Publishers, 1998.

S. D. Ma and A. Gagalowicz. Determination of local coordinate systems for texture synthesis on 3-d surfaces. In *EUROGRAPHICS '85*, pages 109–118. Elsevier Science Publishers, 1985.

J. Malik and P. Perona. Preattentive texture discrimination with early vision mechanisms. *Journal of the Optical Society of America A: Optics and Image Science*, 7(5):923–932, May 1990.

B. Mandelbrot. *The Fractal Geometry of Nature*. W. H. Freeman and Company, 1983.

V. McGee. *Principles of Statistics: Traditional and Bayesian*. Appleton-Century-Crofts, 1971.

T. Meier. Reduction of blocking artifacts in image and video coding. *IEEE Transactions on Circuits and Systems for Video Technology*, 9 (3):490–500, 1999.

B. Meyer and P. Tischer. Compression based refinement of spatial interpolation of missing pixels in greyscale images. In *Proceedings of the 14th International Conference on Pattern Recognition*, volume 2, pages 1274–1277, 1998.

J. Monne, F. Schmitt, and D. Massaloux. Bidimensional texture synthesis by Markov chains. *Computer Graphics and Image Processing*, 17:1–23, 1981.

C. L. Nikias and M. Shao. *Signal Processing with Alpha-Stable Distributions and Applications*. Wiley Inter-Science, 1995.

K. Perlin. An image synthesizer. In *Proceedings of SIGGRAPH 1985*, pages 287–296. ACM Press, 1985.

J. Portilla and E. P. Simoncelli. Texture modeling and synthesis using joing statistics of complex wavelet coefficients. In *Proceedings of the IEEE Workshop on Statistical and Computational Theories of Vision*, 1999. Available: `http://www.cis.ohio-state.edu/~szhu/SCTV99.html` (Accessed: 2000, September 7).

J. Portilla, V. Strela, M. J. Wainright, and E. P. Simoncelli. Image denoising using scale mixtures of Gaussians in the wavelet domain. *IEEE Transactions on Image Processing*, 12(11):1338–1351, 2003.

E. Praun, A. Finkelstein, and H. Hoppe. Lapped textures. In *Proceedings of SIGGRAPH 2000*, pages 465–470. ACM Press, 2000.

W. H. Press, S. A. Teukolsky, W. T. Vetterling, and B. P. Flannery. *Numerical Recipies in C, 2nd edition*. Cambridge University Press, 1992.

L. I. Rudin, S. Osher, and E. Fatemi. Nonlinear total variation based noise removal algorithms. *Physica D*, 60:259–268, 1992.

N. Sebe, M. S. Lew, and D. P. Huijsmans. Toward improved ranking metrics. *IEEE Transactions of Pattern Analysis and Machine Intelligence*, 22(10):1132–1143, 2000.

L. Sjööblom. Swedish accent. *Playboy*, 11:135–141, 1972.

G. Turk. Generating textures on arbitrary surfaces using reaction-diffusion. In *Proceedings of SIGGRAPH 1991*, pages 289–298. ACM Press, 1991.

G. Turk. Texture synthesis on surfaces. In *Proceedings of SIGGRAPH 2001*, pages 347–354. ACM Press, 2001.

VisTex. MIT Vision Texture database. Available: `http://www-white.media.mit.edu/vismod/imagery/VisionTexture/vistex.html` (Accessed: 2002, May 27).

L. Wei and M. Levoy. Fast texture synthesis using tree-structured vector quantization. In *Proceedings of SIGGRAPH 2000*. ACM Press, 2000. Available: `http://graphics.stanford.edu/projects/texture/` (Accessed: 2000, September 7).

L. Wei and M. Levoy. Texture synthesis over arbitrary manifold surfaces. In *Proceedings of SIGGRAPH 2001*, pages 347–354. ACM Press, 2001.

G. Winkler. *Image Analysis, Random Fields and Dynamic Monte Carlo Methods*. Springer, 1995.

S. Wolfram. *A New Kind of Science*. Wolfram Media Inc, 2002.

Y. Xu, B. Guo, and H. Shum. Chaos mosaic: Fast and memory efficient texture synthesis. Technical Report MSR-TR-2000-32, Microsoft Research, 2000.

Y. Y. Yang, N. P. Galatsnos, and A. K. Katsaggelos. Regularized reconstruction to reduce blocking artifacts of block discrete cosine transform compressed images. *IEEE Transactions on Circuits and Systems for Video Technology*, 3(6):421–432, 1993.

P. N. Yianilos. Data structures and algorithms for nearest neighbour search in general metric spaces. In *Proceedings of the 4th Annual ACM Symposium on Discrete Algorithms*, pages 311–321. ACM Press, 1993.

A. Zakhor. Iterative procedure for reduction of blocking effects in transform image coding. *IEEE Transactions on Circuits and Systems for Video Technology*, 2(1):91–95, 1992.

J. Zhang, K. Zhou, L. Velho, B. Guo, and H. Shum. Synthesis of progressively-variant textures on arbitrary surfaces. In *Proceedings of SIGGRAPH 2003*, pages 295–302. ACM Press, 2003.